EFFECT OF INITIAL MOISTURE CONTENT AND SOIL TYPE ON PERMEABILITY OF FROZEN SOIL

A Thesis
Presented in Partial Fulfillment of the Requirements for the
DEGREE OF MASTER OF SCIENCE
Major in Agricultural Engineering

in the
UNIVERSITY OF IDAHO GRADUATE SCHOOL
by

Shang-jau Wang

August, 1969

EFFECT OF INITIAL MOISTURE CONTENT AND SOIL TYPE ON PERMEABILITY OF FROZEN SOIL

A Thesis

Presented in Partial Fulfillment of the Requirements for the

DEGREE OF MASTER OF SCIENCE

Major in Agricultural Engineering

---

in the

UNIVERSITY OF IDAHO GRADUATE SCHOOL

by

Shang-jau Wang

August, 1969

This thesis of Shang-Jau Wang for the Master of Science degree with a major in Agricultural Engineering and titled "Effect of Initial Moisture Content and Soil Type on Permeability of Frozen Soil" was reviewed in rough draft form by each Committee member as indicated by the signatures and dates given below and permission was granted to prepare the final copy incorporating suggestions of the Committee; permission was also given to schedule the final examination upon submission of two final copies to the Graduate School Office:

Major Professor J. L. Bloomsburg Date August 1, 1969

Committee Members [signature] Date August 1, 1969

[signature] Date August 1, 1969

Approval granted by a majority vote of the candidate's Committee at the final examination:

Major Professor _____ Date _____

Reviewed by the Graduate Council; final approval and acceptance is granted:

Graduate School Dean _____ Date _____

BIOGRAPHICAL SKETCH OF THE AUTHOR

Shang-jau Wang was born in Chung-King, Chinese mainland on July 15, 1941. In 1949 he moved with his parents to Kaohsiung, Taiwan, where he received his elementary and secondary education. He later majored in Agricultural Engineering at National Taiwan University, Taipei, Taiwan, and in June, 1965 received his Bachelor of Science degree. After graduation he served in the Chinese Air Force for one year and taught in the Chinese Naval Academy for one year. In September, 1967, he enrolled in the Graduate School of the University of Idaho. He completed the requirements for the Master of Science degree in Agricultural Engineering in August, 1969, of which this thesis is a part.

ACKNOWLEDGMENTS

The author wishes to thank Dr. George L. Bloomsburg of the Agricultural Engineering Department, for the time and energy that he has given so freely in guiding the research and reviewing the thesis.

The advice and constructive criticisms of Professor Calvin C. Warnick, Dr. Myron P. Molnau, and Professor Delbert W. Fitzsimmons are greatly appreciated.

The writer also wishes to acknowledge appreciation for the financial support of the University of Idaho, Water Resources Research Institute provided by the United States Department of Interior, Office of Water Resources Research, as authorized under the Water Resources Research Act of 1964.

TABLE OF CONTENTS

LIST OF FIGURES

FIGURE PAGE

LIST OF TABLES

LIST OF SYMBOLS

A : Cross sectional area perpendicular to the direction of heat flow.

a : Diffusivity constant - L^2/t.

a_f : Diffusivity coefficient in frozen soil - L^2/t.

a_u : Diffusivity coefficient in unfrozen soil - L^2/t.

C : Relative water content - dimensionless.

C_f : Volumetric heat of frozen soil - $Btu/L^{3o}F$.

C_h : Volumetric heat of soil - $Btu/L^{3o}F$.

C_{iw} : Interfacial energy constant - F/F.

C_u : Volumetric heat of unfrozen soil - $Btu/L^{3o}F$.

D_o : The value of diffusivity when $\theta = \theta_o$ - L^2/t.

$\bar{D}$: Weighted-mean diffusivity - L^2/t.

D_{pt} : Threshold density of compacted wet snowpack in percent.

D_{so} : Density of initial dry snowpack in percent.

D_{st} : Threshold density of dry snow in compacted wet snowpack in percent.

$D(\theta)$: The soil water diffusivity - L^2/t.

F : Free energy or energy available - LF.

F_t : Freezing index - ^oFt.

g : The rate of water migration into the frozen soil - M/tL^2.

H_s : Soil suction - E/L^3.

i : Thermal gradient - $^oF/L$.

k_a : Permeability as determined by air flow - L^2.

k_h : Thermal conductivity - Btu/tL^oF.

k_{hf} : Thermal conductivity of frozen soil - Btu/tL^oF.

k_{uf} : Thermal conductivity of unfrozen soil - $Btu/tL^{o}F$.

L_h : Latent heat of the pore water - $Btu/L^3\ ^{o}F$.

L : Length of soil column - L.

P : Pressure - F/L^2.

P_a : Atmospheric pressure - F/L_2.

P_d : Snowpack depth in percent of initial depth.

P_{iw} : Ice-water interfacial pressure - F/L^2

P_w : Accumulated water content in percent of initial water content.

Q : Cumulative flow of water - M/L^2.

q : Velocity of fluid flow - L/t.

Q_h : Heat transfer - Btu/t.

q_h : Unit area heat transfer - Btu/tL^2.

r : Principle radius of curvature of curved interface - L.

S : Saturation - dimensionless.

S' : Slope of $\log_{10}y$ versus time curve - dimensionless.

S_p : Specific heat - $Btu/M^{o}F$.

T : Temperature.

T_f : Temperature below freezing.

t : Particular instant of time.

u : Btu/L^3.

V : Volume - L^3.

V_a : Volume at atmospheric condition - L^3.

W : Boltzman transformation - dimensionless.

x : Spatial coordinate - L.

y : Spatial coordinate - L.

γ_d : Dry density of the soil - M/L^3.

θ : Water content - M/L^3.

θ_o : The constant water content at the boundary x=0 - M/L^3.

θ_i : The initial water content - M/L^3.

λ : Correction coefficient.

μ : Viscosity - Ft/L^2.

ϕ : Porosity - dimensionless.

ω : Water content - dimensionless.

ABSTRACT

The purpose of this thesis was to investigate the factors which affect the permeability of frozen soil, especially the effect of soil type and initial moisture content before the soil is frozen. This information is necessary to be able to predict when the possibility of frozen ground floods exists.

The permeability of frozen soil columns was measured under isothermal conditions in the laboratory using air. The product of porosity and 1.0 minus the initial moisture content was determined to be a significant parameter affecting the permeability to air. When this parameter is less than 0.13 the permeability approaches zero in all types of soils tested. Using certain critical values of the parameter would enable a person to predict when the possibility of frozen ground floods exists by taking soil samples in the field. The particular critical value of $\emptyset(1-S)$ to be used for various soils should be investigated in field studies.

CHAPTER I

INTRODUCTION

Research work on frozen ground floods was originally started at the University of Idaho in 1965 by A. C. Robertson. This type of flood is quite common in many areas of the Northwest during the winter and early spring months. The U. S. Army Engineers reported (1966) that some of the worst of these floods that have occurred in recent years were those during the winters of 1962 and 1964 in southeastern Idaho in which there was extensive damage, loss of income and suffering of the flood plain population in general.

The precipitation pattern of this area is largely determined by topography; climatic regimes range from semi-arid in the low elevation plain area to semi-humid in high mountain areas. Usually floods in southeastern Idaho are of three general types:

1. Spring melt of head-water snow, which may be augmented by rain.
2. Localized flooding from high intensity summer precipitation.
3. Rain on frozen ground which may be augmented by low elevation snowmelt.

In the upper Snake River Basin most floods are of Type 1; that is, they are generated by spring snowmelt floods since the snow over most of this high elevation area is so deep that winter rain is

either absorbed or considerably impeded.

Flood peaks of Type 3 caused by rain on frozen ground are more characteristic of the Portneuf River basin. Although considerably more than half of the annual flood peaks in the Portneuf River during the period of record at Pocatello are primarily from high elevation snowmelt, several large floods of record have been caused by rain on frozen ground.

Streamflow records on the tributaries south of the Snake River and west of the Portneuf basin to the Bruneau basin indicate maximum flow peaks have been generated by all three flood types. However, it appears that the greatest potential for major floods in the lower reaches of the streams is from a winter rain on frozen ground augmented by snowmelt.

The depth and areal extent of the frozen ground were two of the most important causes of the floods. Preflood conditions were ideal for development of the frozen ground conditions, with August 1961 precipitation somewhat above normal and September and October precipitation well above normal throughout the region. This, coupled with below-normal temperature during the same period, provided an excellent chance for any soil moisture deficiencies to be made up.

From the fall season into the winter months of November, December and January, precipitation was generally above normal and temperatures below normal throughout the region. There were alternating periods of thawing and freezing. Precipitation that fell at lower elevations where there was no snow cover percolated into the

ground and became frozen. At the higher elevations where the snow pack formed a layer of insulation the ground remained unfrozen. In the areas above 6,500 feet which were apparently unfrozen, the snow cover and the ground apparently absorbed most of the excess water.

PURPOSE OF STUDY

A relationship often discussed in hydrologic studies is that runoff equals precipitation minus infiltration and storage. In the case of winter floods, the infiltration may be small due to frozen ground while the total water available for runoff may be greater than the precipitation during any one storm because of the snow pack.

It is the purpose of this thesis to investigate the factors which affect the infiltration rate for frozen ground. Specifically, the effect of soil type and initial moisture content on the permeability was investigated.

CHAPTER II

LITERATURE REVIEW

When rain occurs on snow some of it is held in the snow much as water is held in sand. If there is enough rain it will eventually flow through the snow to the ground surface. Some will then infiltrate (depending on the infiltration rate) while the remainder will tend to run off as over-land flow. There can be melting of the snow or freezing of water during this time.

Many factors influence the rate at which water will move into frozen soil. Five of the factors will be considered. The type of snow structure influences the rate at which liquid water moves through the snowpack and is available for infiltration. The type of frost, the soil temperature, the rate at which the moisture moves to the freezing front and the formation of frost in the soil are interrelated factors which determine the rate at which the frozen soil will accept water from the rainfall and from the snowpack.

EFFECT OF SNOW STRUCTURE

Often frozen ground is covered with snow. The water available for infiltrating into the frozen soil depends on the snowmelt and water movement through the snowpack. However, different snow types allow different rates of snowmelt and different rates of water movement through the snowpack.

There have been many articles written concerning the transmission

rate of water through snow. Gerdel (1954) stated that Oeschim measured the moving front of fuchsine-dyed water through columns of new and compacted snow and found that the transmission rate was highest through low density snow. Gerdel also found that a coarse-grained natural spring snow pack of high density has a much different structure and greater permeability than an artificially compacted new snow of the same density. A ripe snow will not retain much more than 2 percent liquid water for more than a few hours. A liquid water retention capacity of 2 percent in a ripe pack of 0.4 gm/cm^3 density is equivalent to about 0.1 inch of water per foot of snow, about the same as the field moisture capacity of a sandy soil. It was pointed out that density values between 0.25 and 0.50 gm/cm^3 for ripe snow packs have been reported in the literature.

Although the snow pack is somewhat like a coarse sand in its capacity to hold or transmit water, the transmission rate and field capacity of a sand profile will vary little from time to time whereas the transmission rate of snow may increase as rain or melt water moves through the pack

By using a snow moisture capacitance meter which makes use of the difference in the dielectric constants of ice and water, Gerdel (1954) found that the transmission rate of water through snow of 0.35 to 0.46 gm/cm^3 density may vary from 0.9 to 24 inches per minute. The higher transmission rates appear to be associated with high density and a ripe pack structure.

A snow pack may have a temporary high water storage capacity

pending the development of flow channels within the pack or over the ground beneath the pack and pending the satisfaction of the moisture holding capacity of the snow. Drainage glands or pipes develop within the pack and flow channels develop at the contact with the ground surface very rapidly. When the drainage network is established within the pack and its water holding capacity is satisfied, the discharge of melt or rain water will be approximately equal to the rate at which the liquid phase is available at the surface of the snow. However, the delay in development of channels does allow infiltration into the ground because the snow-cover tends to keep the ground unfrozen. Gold (1967) reported that snow cover had the effect of adding to the soil surface an insulating layer whose depth varied with time and whose thermal conductivity was usually lower than that of the soil. The snow cover was therefore primarily responsible for the fact that the average soil surface temperature in winter was about 6 to 11°C warmer than the average air temperature. Some data from Gold (1963) showing the variation in ground temperature, air temperature and snow depths are shown in Figure 1.

G. A. Morozov (1967) reported that the structure and density of the snow cover are the main characteristics determining the mechanical and thermophysical properties of snow which must be taken into account when computing the depth of soil freezing. He also stated that the transfer of water vapor in the snow cover leads in time to changes in the structure and density of the snow.

When there is rainfall on snow, some of the snow will melt

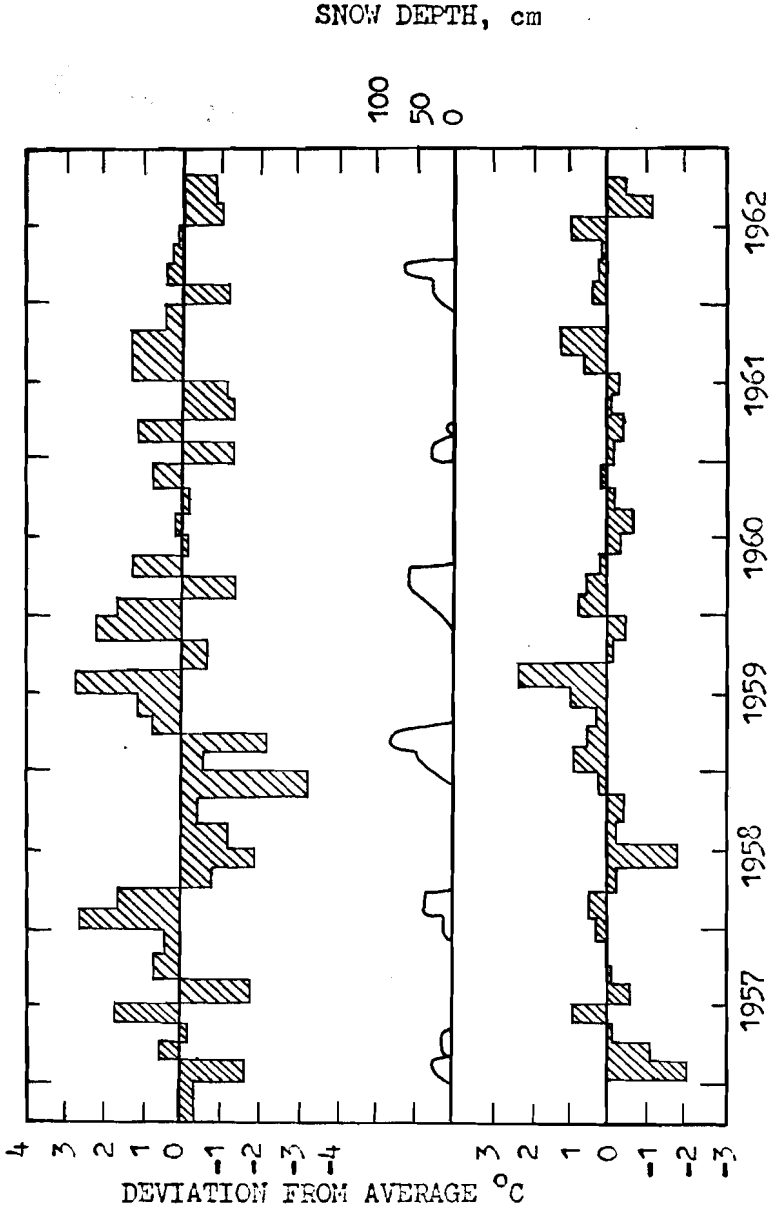

Fig. 1 - Time dependence of deviation of 50-day average air and 10-cm ground temperature from 6-year average.

and the surface runoff will increase. A computational procedure for predicting runoff from a rain-on-snow storm using the concept of a threshold density was developed originally by the U. S. Army Corps of Engineers. This concept has been expanded to recognize the shrinking of the snowpack as water is added.

Frederick (1966) reported that Garstka, Grout, Miller, and Monfore (1951) of the U. S. Bureau of Reclamation conducted a laboratory experiment to evaluate the compaction resulting from added water. The procedures they used were: The fresh snow, which had fallen at approximately $0^{\circ}F$ the night before, was shoveled into a large plexiglass cylinder. This cylinder full of snow was set in a pan and placed on a weighing scale in a controlled temperature cold room. Cold water was sprinkled on top of the snow column in 1-pound increments, and the shrinkage of the snow was observed.

Some of these tests are summarized in Figure 2 in which the depth of snowpack in percent of initial depth is plotted versus the initial water content. After the cylinder was filled outdoors, the snow had a density of 15.4 percent. This point is plotted at 100 percent depth and 100 percent water content. During the time the sample was moved indoors, the snow compacted to 87 percent of depth and the density to 17.7 percent. As water was added the snow continued to compact, as indicated by the decreasing percentage of depth for each of the points. By the time the water content was 177 percent of the initial water content, the depth was 64 percent of the

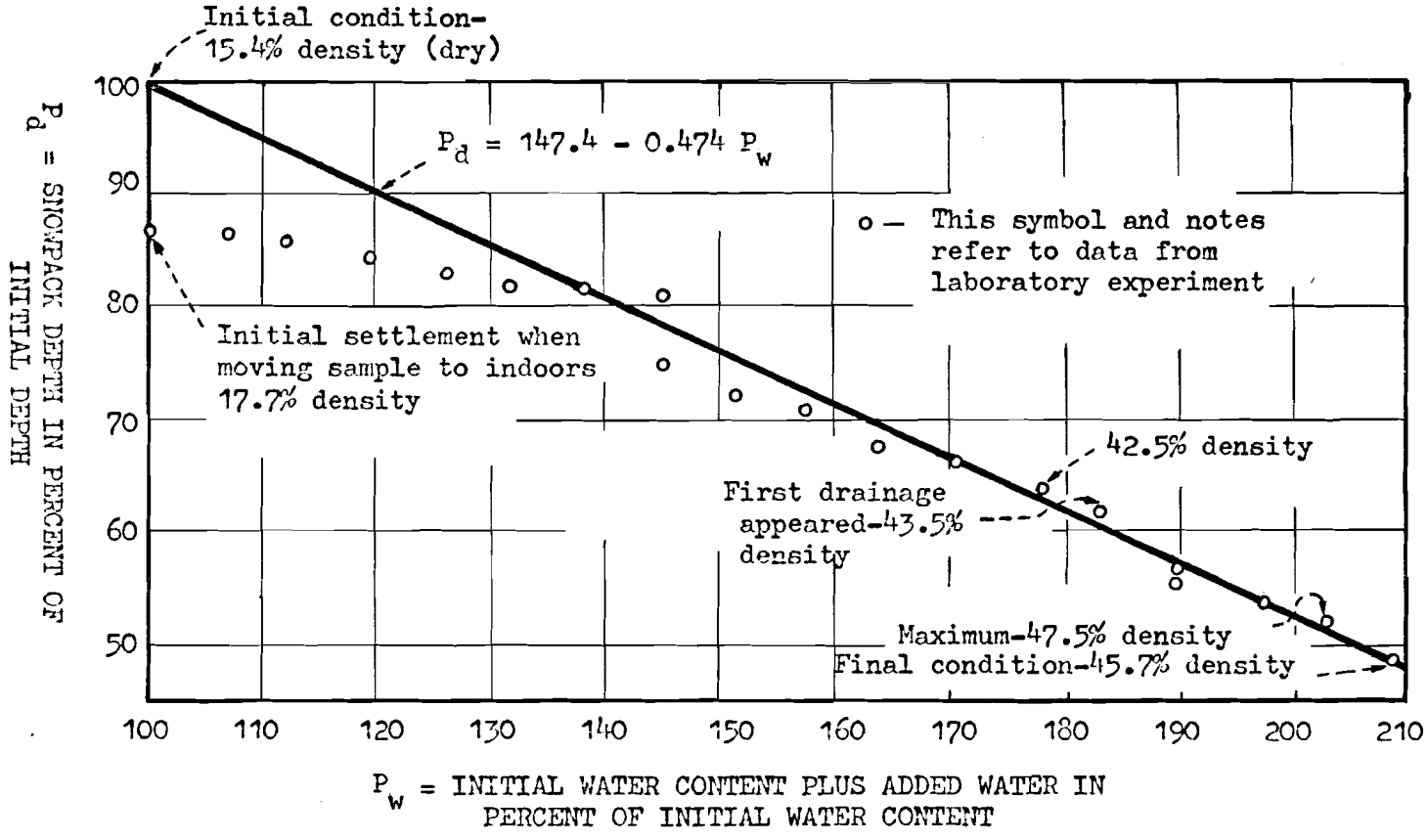

Fig. 2 - Decrease in snowpack depth due to addition of water.

original depth and the density was 42.5 percent. Prior to this point in the test, the added water was retained in the snow.

Drainage of water from the bottom of the snow column was first observed at the next point when the density was 43.5 percent. During the test, water was added until no further compaction took place, and after the excess water was allowed to drain out, the final density was 45.7 percent. The relationship between depth and accumulated water is represented by a straight line having the equation:

$$P_d = 147.4 - 0.474\ P_w \qquad (1)$$

where:

P_d is snowpack depth in percent of initial depth,

P_w is accumulated water content in percent of initial water content.

It was assumed in the test that the snowpack is homogeneous and free water in the snowpack is distributed evenly throughout the depth of the pack. No compaction takes place after the threshold density has been reached. Threshold densities range from 40 to 45 percent. It was observed that drainage occurs only after the snowpack has reached its threshold density.

The conditions of the snowpack at the adopted threshold density can be computed from the following equations:

$$P_w = 147.4\ D_{pt} / (D_{so} + 0.474\ D_{pt}) \qquad (2)$$

$$P_d = 147.4\ D_{so} / (D_{so} + 0.474\ D_{pt}) \qquad (3)$$

$$D_{st} = 0.678 \left(D_{so} + 0.474 D_{pt} \right) \qquad (4)$$

where:

D_{so} is density of initial dry snowpack in percent,

D_{pt} is threshold density of compacted wet snowpack in percent,

D_{st} is threshold density of dry snow in compacted wet snowpack in percent.

For calculating the depth of snowpack and drainage from snowmelt knowledge or assumption of initial and subsequent basic data is required. In succeeding intervals of time, the precipitation in inches of water must be known. If this precipitation falls as snow its density must be known. The potential snowmelt during each interval may be computed by an empirical snowmelt equation developed by the U. S. Army Corps of Engineers (1960).

For computing the runoff from snowmelt, it is generally necessary to separate a drainage basin into elevation zones and compute the runoff separately for each zone. The division of the basin area into zones according to elevation permits the use of different initial snow conditions for each of the elevation zones. Also, the wind speed, temperature, and the factors producing drainage and the time of runoff may vary considerably from zone to zone.

TYPES OF SOIL FROST

Different types of soil frost may be formed due to differences in the physical or chemical properties of soil. The continuous change of air temperature can also affect the type of soil frost.

The permeability and storage of frozen soil depend largely on the types of soil frost.

It was reported by Trimble, Sartz, and Pierce (1958) that the infiltration rate depends to a considerable extent on the type of soil frost. Four terms, concrete, granular, honeycomb, and stalactite, have been used to describe the structure or type of soil frost.

Concrete frost is characterized by an extremely complex formation of a great many thin ice lenses, with the ground surface being very hard, like concrete. This kind of frost usually forms in bare agricultural land.

Granular frost is often found in woodland soils that contain organic matter. It consists of small frost crystals intermingled with the soil particles. These grains aggregate around the soil particles but remain separate from each other. Those are easily broken up.

Honeycomb frost has a loose, porous structure resembling honeycomb. It is very often found in highly aggregated soils.

Stalactite frost consists of loosely fused, columnar ice crystals. It often forms in bare ground where the surface is saturated.

Haupt (1967) considered two dominant types of soil frost -- stalactite and porous concrete.

Alternate freezing and thawing probably form these frost types in the following manner. Rapid daytime melting of a shallow snowpack saturates 1 to 2 inches of the surface soil and forms the loosely fused, columnar stalactite ice crystals. As these crystals enlarge

at night, they heave the surface soil and form an irregular pattern of small columns. But when the shallow snowpack disappears, the exposed surface layer thaws and gradually dies out. These phenomena, together with refreezing at night, cause large crystals to reform into the small, crystalline structure of the porous concrete type. Very slow or intermittent daytime melting of a snowpack causes both frost types to coexist. On the other hand subfreezing daytime temperatures probably favor development of porous concrete frost.

Stalactite frost, with its rough and very porous microrelief, absorbs rainfall-snowmelt literally like a sponge. The lack of overland flow associated with this frost type substantiates other findings that indicate that certain types of frozen soil actually cause an increase of infiltration rate.

A granular type of frost, found typically in eastern woodland soils has been reported by Trimble, Sartz and Pierce (1958) as more permeable than unfrozen soil.

According to Haupt (1967), porous concrete frost reduces the infiltration capacity so that overland flow is increased on burned or sparsely vegetated sites relatively free of exposed rock if the rainfall intensity exceeds 3 inches per hour.

Usually, as stalactite frost melts, the infiltration rate decreases; but as the denser porous concrete frost melts, water intake increases.

When soil is frozen, snow cover and its cooling effect on rainwater tend to preserve soil frost in its original form and to

keep it visibly intact during a storm by a substantial heat transfer from rainwater to the snow matrix. After the snow melts completely, direct exchange of heat between rain and frozen soil takes place; then the frost breaks down and a mud veneer is formed. During a rainstorm, persistence of snow cover over porous concrete stalactite frost prevents overland flow.

MOISTURE MOVEMENT DURING FREEZING

The formation of different types of ground frost in winter is partially due to moisture movement to the freezing front. This movement is different for different kinds of soil with different moisture contents. The dependency of moisture movement on the time and temperature can be theoretically analyzed.

The physics of moisture movement in porous media under temperature gradients has been described in many articles. Smith (1943) supposed that moisture movement for hot to cold occurs partly in the liquid phase; but this hypothesis was not supported by data offered by Gurr, Marshall and Hutton (1952).

The existence of large temperature gradients in the air voids was experimentally measured by Woodside and Kuzmak (1958) on a large scale model. Cary (1963) later applied the theory of nonisothermal diffusion of water vapor to vapor transport under a temperature gradient across an air gap. Dirksen (1964) indicated that the process of moisture movement is considerably altered by the presence of an ice phase in a porous medium. The direction of water flow can be

predicted in an isothermal system by macroscopic quantities such as tension and water content but in a nonisothermal system the temperature difference must be considered also.

Hoekstra (1967) reported that in the unfrozen soil all the water is in the liquid form. In the frozen soil some of the water is in the form of ice and some in the form of unfrozen water. Any additional water that moves to a particular location does not increase the thickness of the unfrozen film but freezes to ice. The amount of unfrozen water is determined by the temperature at that location. The water content at the freezing front is the amount of unfrozen water. From Figure 3 it is clear that in the frozen soil the "liquid water content" depends on temperature only.

Gardner (1959) discussed solutions for flow equations for water in porous media for the drying of soils. One can make use of Gardner's treatment to derive some pertinent equations for the cumulative transport of water from the unfrozen into the frozen soil.

As boundary conditions, Gardner (1959) used a uniform initial water content and a constant water content at the boundary of a semi-infinite column. A constant water content boundary is equivalent to a constant tension boundary, if one assumes a unique relation between water content and tension in a soil.

These boundary conditions of uniform initial water content and a constant water content at the boundary approximately correspond to the water movement to a freezing front, especially in the case where the freezing front remains at the same position. Following Gardner's

treatment one can proceed to derive some pertinent equations for the cumulative transport of water from the unfrozen into the frozen soil.

The diffusivity equation for water in soil has been written as:

$$\frac{\partial \theta}{\partial t} = \frac{\partial}{\partial x}\left[D(\theta) \frac{\partial \theta}{\partial x} \right] \qquad (8)$$

where:

θ is water content,

$D(\theta)$ is the soil water diffusivity,

x is a horizontal coordinate,

t is time.

The boundary conditions discussed above correspond to:

$\theta = \theta_i$, $\quad x > 0$, $\quad t = 0$

$\theta = \theta_o$, $\quad x = 0$, $\quad t \geq 0$

where:

θ_i is the initial water content,

θ_o is the constant water content at the boundary $x = 0$.

Substitution of the Boltzman transformation, $W = x/2\sqrt{D_o t}$ into equation (8) reduces it to an ordinary differential equation of the form,

$$-2W\left(\frac{d\theta}{dW}\right) = \frac{d}{dW}\left[\frac{D(\theta)}{D_o} \cdot \frac{d\theta}{dW} \right] \qquad (9)$$

with the boundary conditions,

$\theta = \theta_1$, $\quad W \longrightarrow \infty$

$\theta = \theta_o$, $\quad W = 0$

D_o is the value of diffusivity when $\theta = \theta_o$. In the experiment under consideration, θ_o can be considered the unfrozen water content at the freezing front. The water will migrate into the frozen soil at a rate g, given by;

$$g = D_o \left[\frac{d\theta}{dx} \right]_{x=0} \qquad (10)$$

A relative water content C, is defined by,

$$C = \frac{\theta - \theta_o}{\theta - \theta_o}$$

However,

$$\frac{dC}{d\theta} = \frac{1}{\theta_1 - \theta_o} \quad ; \text{ and } \frac{dW}{dx} = \frac{1}{2\sqrt{D_o t}} \quad ,$$

so we can write,

$$\frac{d\theta}{dx} = \frac{dW/dx}{dC/d\theta} \cdot \frac{dC}{dW} = \frac{\theta_1 - \theta_o}{2\sqrt{D_o t}} \cdot \frac{dC}{dW} \quad .$$

Substituting this expression into equation (10) when x = 0, W = 0, we get,

$$g = \frac{1}{2}\sqrt{\frac{D_o}{t}}\,(\theta_1 - \theta_o)\left(\frac{dC}{dW}\right)_{W=0} \qquad (11)$$

If a weighted-mean diffusivity, $\bar{D}$ is defined as

$$\bar{D} = \frac{\pi}{4} D_0 \left(\frac{dC}{dW}\right)^2_{W=0} \tag{12}$$

equation (11) reduces to,

$$g = (\theta_1 - \theta_0)\sqrt{\frac{\bar{D}}{\pi t}} \tag{13}$$

Equation (13) can be used to characterize the flow of unfrozen water into the frozen soil. The cumulative flow of the water moving from the unfrozen into the frozen region is given by,

$$Q = \int_0^t g\, dt = 2(\theta_1 - \theta_0)\sqrt{\frac{\bar{D}}{\pi}} \cdot \sqrt{t} \tag{14}$$

Thus, when the freezing front remains at the same position the cumulative water transport into the frozen part of the soil column is proportional to the square root of time, and is independent of the manner in which $\bar{D}$ depends upon θ .

In Figure 4, the cumulative water movement from the unfrozen into the frozen soil is plotted versus the square root of time. The points on the graph represent the cumulative water movement at the time indicated on the curves of Figure 6. The results agree well with the derived equation (14). From equations (11), (12), and (13) the diffusivity of the water content at the freezing front can be

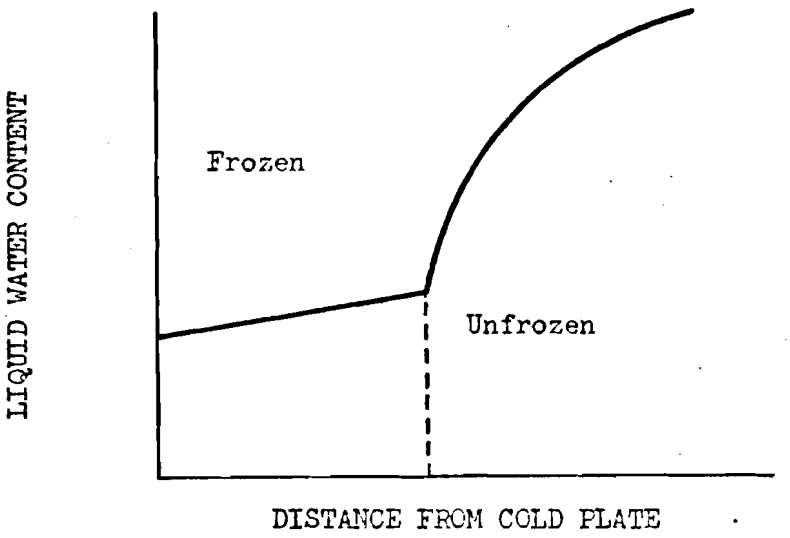

Fig. 3 - The "liquid water content" as a function of distance from the cold plate. In the frozen part of the soil ice is also present.

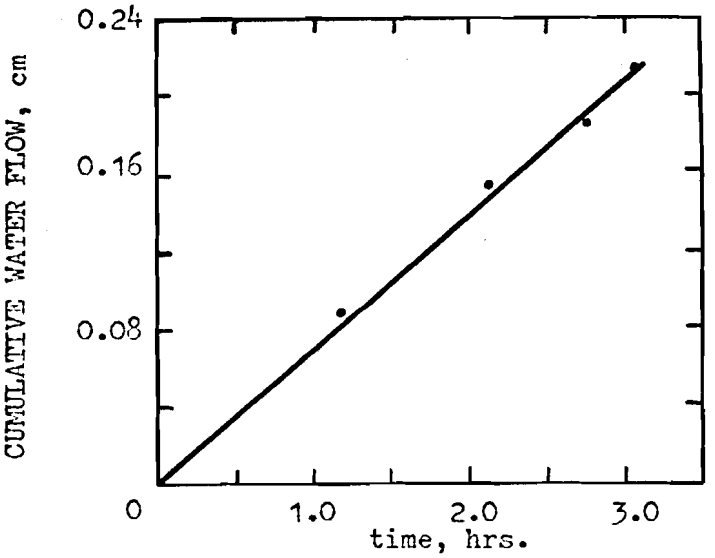

Fig. 4 - Cumulative water transport from the frozen into the unfrozen part of the soil.

evaluated from the slope of the line in Figure 4.

In Figure 5 the water content versus time and temperature are shown at 2 inches from a cold plate. In the experimental work the cold plate temperature is $-10^{\circ}C$. If the pores become filled with ice, ice lens formation can be expected to take place.

Figure 5 shows that the water content first decreases, but when the freezing front reaches a particular location the moisture content starts to increase.

The same situation can be expressed as shown in Figure 6 where the water content is plotted as a function of distance from the cold plate. The cold plate temperature was $-5^{\circ}C$ and the initial water content 0.266 g/cm^3. The breaks in the curves indicate the boundary between frozen and unfrozen soil. The freezing front after 1.44 hours became relatively stable and progressed less than 1 cm during 9 hours.

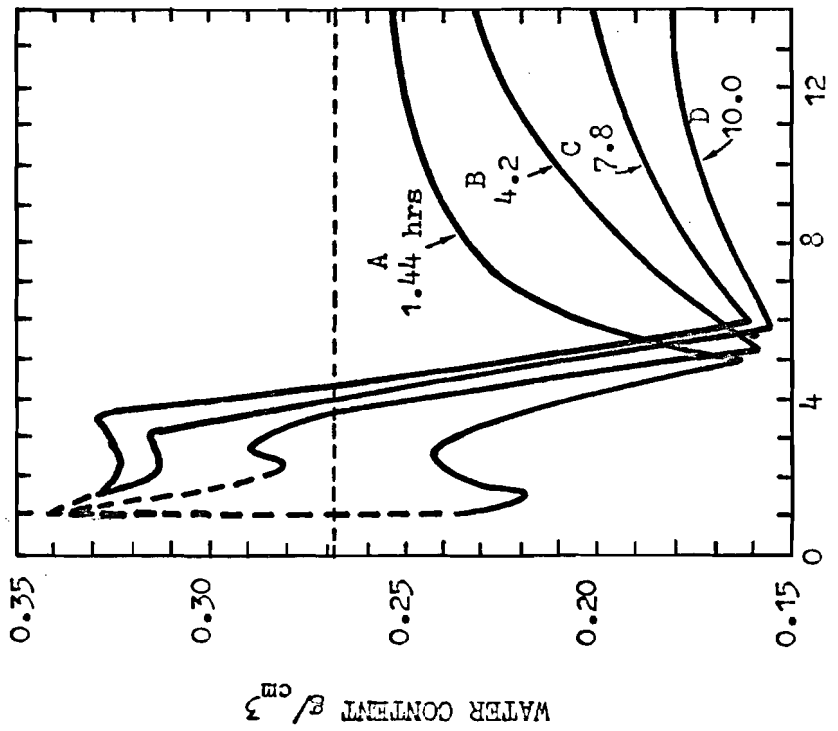

Fig. 6 - Water content profiles at different times.

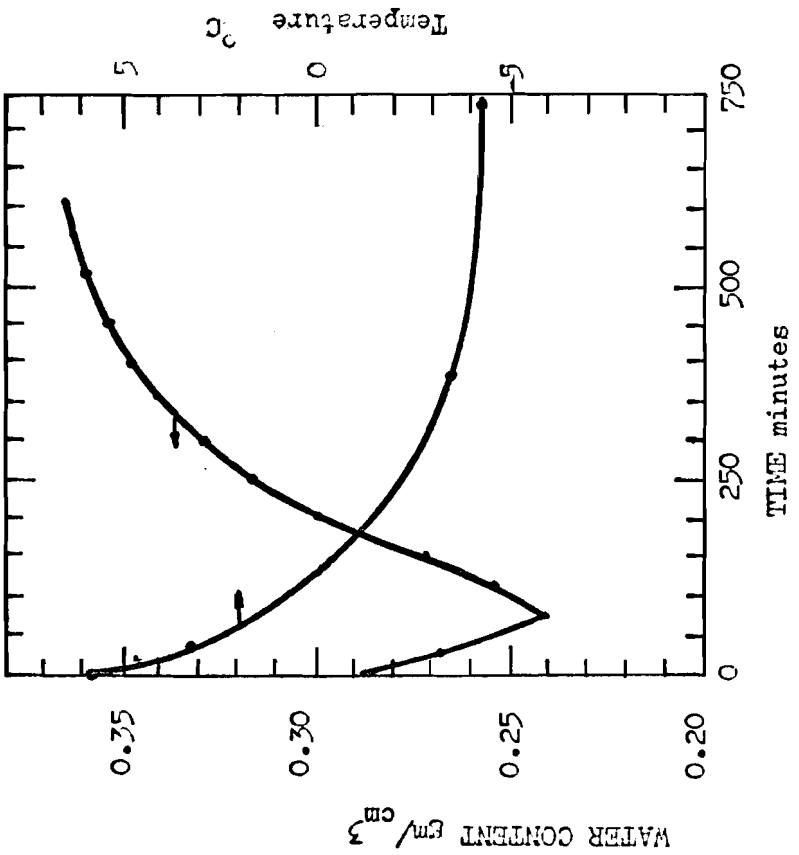

Fig. 5 - Water content and temperature versus time at 2 inches from the cold plate. Cold plate temperature -10°C

CHAPTER III

FUNDAMENTAL CONCEPTS

Frost develops in the soil due to heat movement upward toward the cold soil surface. The problem of the temperature distribution in the soil is therefore associated with a one-dimentional heat flow problem. An analysis of this problem will be considered as well as the actual formation of ice crystals and the measurement of the permeability of frozen soil under temperatures below freezing.

TEMPERATURE DISTRIBUTION

The variation of temperature with depth below the soil surface may be plotted for any particular time. Examples of this are shown in Figures 7 and 8 as given by Terzaghi (1952). Two conditions of the frost front are shown; these are an active layer and an active layer with a permafrost layer.

It was reported by Yong and Warkentin (1966) that the variation of soil temperature with time can be plotted to show the intensity of temperature. Since there is a local fluctuation in temperature between day and night, the mean daily temperature is used. The temperature intensity is the area under the curve in Figure 9. The temperature intensity, considered in terms of degree days below freezing, determines the penetration of the frost front. The mean daily temperature is plotted for a period of one year. The freezing index, F_t, is the shaded area defined by the temperature curve. If

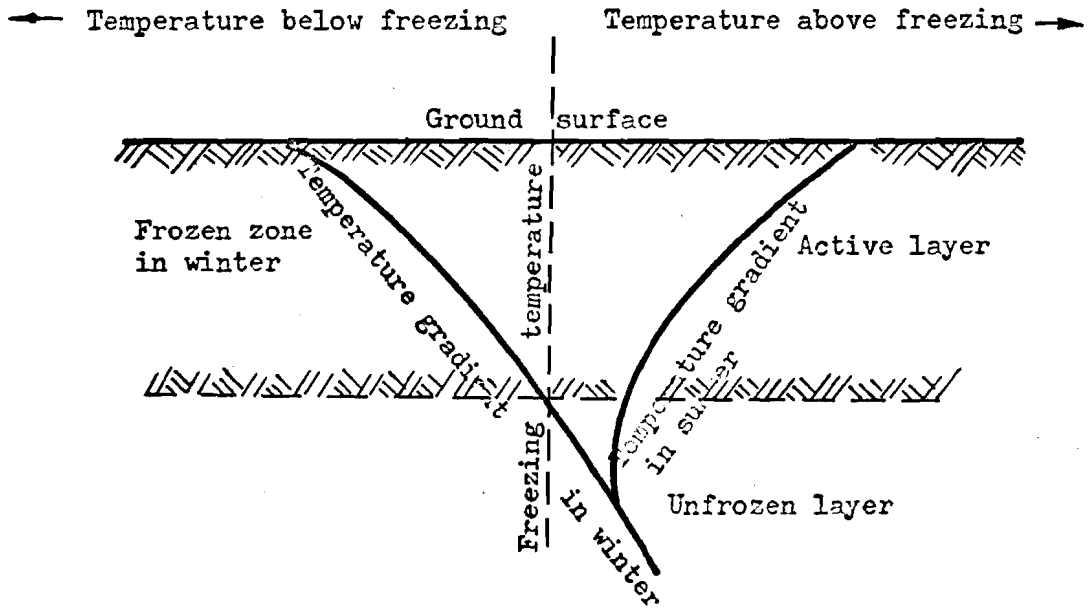

Fig. 7 - Ground temperature profile showing:
Active layer only

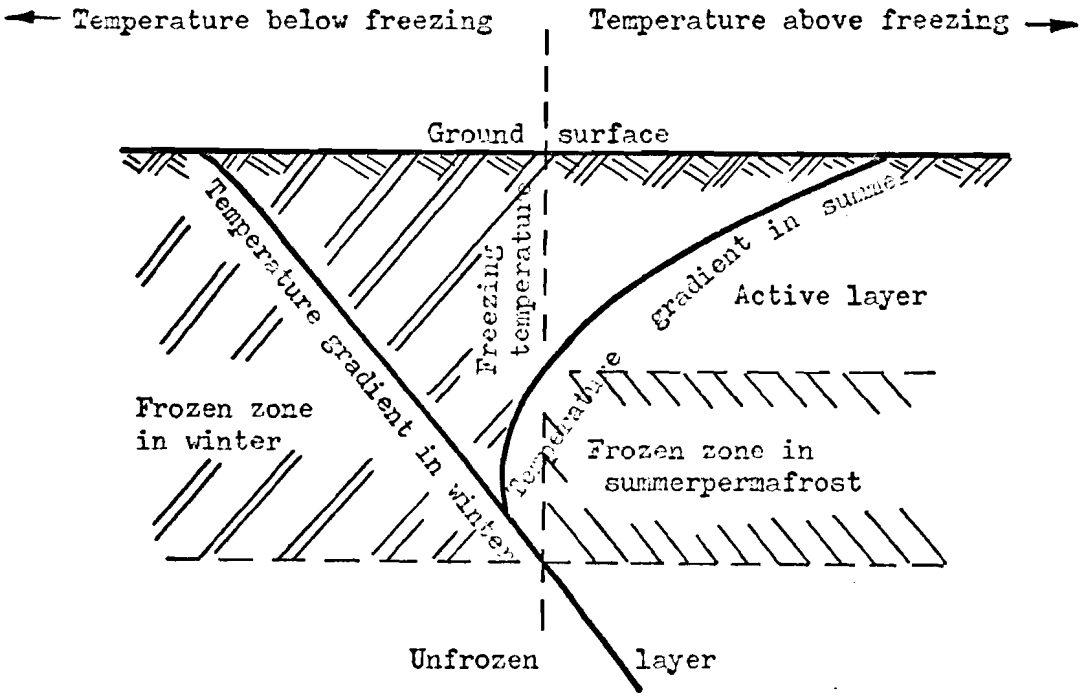

Fig. 8 - Ground temperature profile showing:
Permafrost and active layer

T_f represents the mean surface temperature during the freezing period t, then the freezing index F_t is T_f x t degree days. It is evident that the higher F_t is, the greater will be the frost penetration.

Yong and Warkentin also reported that the frost penetration, or the depth of the frost front into the subsoil depends on several factors.

1. Freezing index and associated temperature factors.
2. Soil type and grain-size distribution.
3. Thermal properties of the soil-water system.
   a. Specific heat of mineral particles.
   b. Volumetric heat of the system.
   c. Latent heat of the pore water.
   d. Thermal conductivity of the soil.
4. Nature of the pore water.

The specific heat represents the quantity of heat required to raise the temperature of a unit mass of material one degree (Fahrenheit or Centigrade). The volumetric heat depends on the specific heat and can be obtained by multiplying the specific heat by the dry density of the material. This is different for frozen and unfrozen soils. Using values of S_p for water and ice as 1.0 and 0.5 Btu/lb/^{o}F respectively, the volumetric heats for frozen and unfrozen soil may be calculated. If C_u is the volumetric heat of unfrozen soils then,

$$C_u = \gamma_d S_p \text{ (soil particles)} + \frac{\omega}{100} \gamma_d S_p \text{ (water)}. \quad (15)$$

For clay we have,

S_p (soil particles) = 0.17

and S_p (water) = 1.0

Therefore,

$$C_u = \gamma_d (0.17 + \frac{\omega}{100})$$

In the above equations,

S_p is specific heat Btu/lb/^oF

γ_d is dry density of the soil, lb/ft^3

and ω is water content, lb of water/lb of dry soil.

For frozen soils, C_f is the volumetric heat, so that,

$$C_f = \gamma_d S_p \text{ (soil particles)} + \frac{\omega}{100} \gamma_d S_p \text{ (ice)}, \quad (17)$$

or

$$C_f = \gamma_d (0.17 + \frac{0.5\omega}{100}). \quad (18)$$

The heat content and change in thermal energy of a soil-water system as it freezes or thaws depend on C_u, C_f, and L_h. The relationship between these factors is shown in Figure 10. The thermal energy change is linear with temperature both below and above freezing but interrupted by the latent heat of fusion L_h, of the pore water at the freezing point.

In the so-called Stefan model of the temperature distribution, it is assumed that the variation of temperature from the top of the ground surface to the frost line is linear, and that the temperature remains constant below the frost line. This is shown in Figure 11.

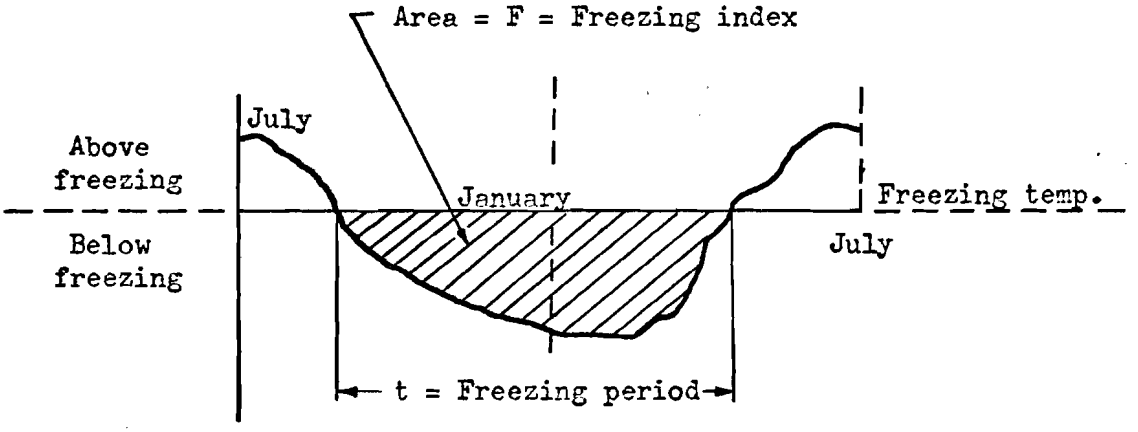

Fig. 9 - Freezing index from annual variation in surface temperature.

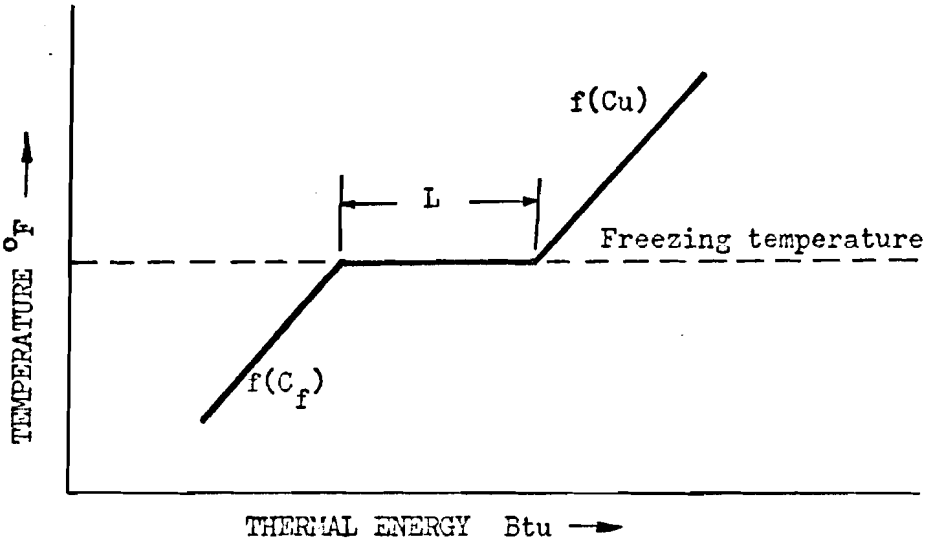

Fig. 10 - Heat content or thermal energy diagram for an idealized soil-water system.

The heat flow for this model can be calculated as follows: By the principle of conduction,

$$q_h = -k_h \frac{\partial T}{\partial y} \tag{19}$$

$$Q_h = k_h i A \tag{20}$$

$$= k_h \frac{T_a - T_b}{y} A,$$

where:

Q_h is heat transfer,

i is thermal gradient,

k_h is thermal conductivity,

A is area,

$q_h = Q_h/A$

y is depth taken as downward from the top of the ground surface.

At a point "A" on the frost front, the equation of continuity must be satisfied. This requires that the latent heat released as the pore water freezes to a depth Δy in time Δt be equal to the rate of heat conduction to the ground surface. For small values of Δy and Δt this may be written as,

$$k_{hf} \frac{T_f}{y} = L_h \frac{dy}{dt}, \tag{21}$$

where:

T_f is temperature below freezing as shown in Figure 11,

and L_h is latent heat of the pore water.

Rearranging and integrating

$$\frac{K_{hf}}{L_h} T_f dt = y dy,$$

$$\frac{K_{hf}}{L_h}\int T_f dt = \frac{y^2}{2} ,$$

therefore

$$y = \sqrt{\frac{2K_{hf}\int T_f dt}{L_h}} . \qquad (22)$$

The term $\int T_f dt$ in degree hours is equal to the freezing index F_t in degree days times 24. This gives,

$$y = \sqrt{\frac{48K_{hf}F_t}{L_h}} \qquad (23)$$

This equation is called the Stafen equation since it is developed from the model shown in Figure 11.

It has been found that prediction of the depth of frost penetration y made on the above basis tends to overestimate the actual penetration, and a development by Aldrich (1956) is sometimes used.

From the theory of the conservation of thermal energy, it can be shown that

$$\frac{\partial u}{\partial t} + \frac{\partial q}{\partial y} = 0 , \qquad (24)$$

where u is thermal energy, Btu/ft^3,

Since

$$du = C_h dt , \qquad (25)$$

where C_h is volumetric heat of soil,

then

$$\frac{\partial u}{\partial t} = C_h \frac{\partial T}{\partial t} \quad . \tag{26}$$

Differentiating equation (19), we get,

$$\frac{\partial q}{\partial y} = -k_h \frac{\partial^2 T}{\partial y^2} \quad . \tag{27}$$

Substituting equations (26) and (27) into equation (24),

$$\frac{\partial T}{\partial t} = \frac{K_h}{C_h} \frac{\partial^2 T}{\partial y^2} \quad . \tag{28}$$

Defining k_h/C_h as "a", the diffusivity constant, the equation can be written as,

$$\frac{\partial T}{\partial t} = a \frac{\partial^2 T}{\partial y^2} \quad . \tag{29}$$

The above equation is the diffusion or heat flow equation, which represents the temperature profile in the subsoil at any instant of time.

The use of the diffusion equation provides an estimation of frost penetration and the temperature distribution as shown in Figure 12. The soil temperature profile is for any time "t".

In the frozen soil layer, the ground temperature profile is given by the diffusion equation as

$$\frac{\partial T_f}{\partial t} = a_f \frac{\partial^2 T_f}{\partial y^2} \quad . \tag{30}$$

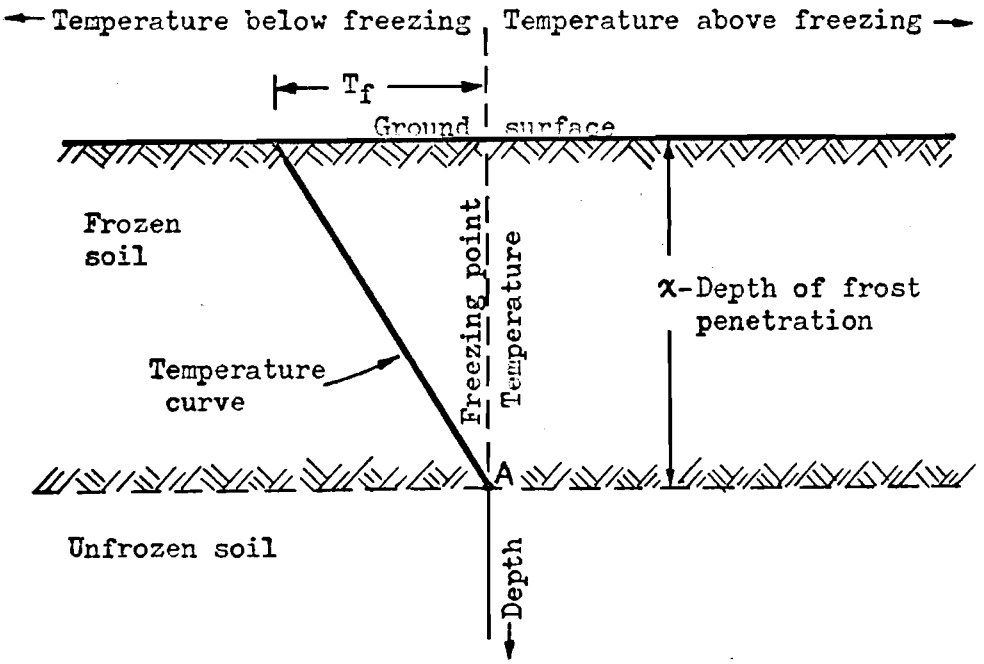

Fig. 11 - Thermal conditions assumed for the Stefan Model.

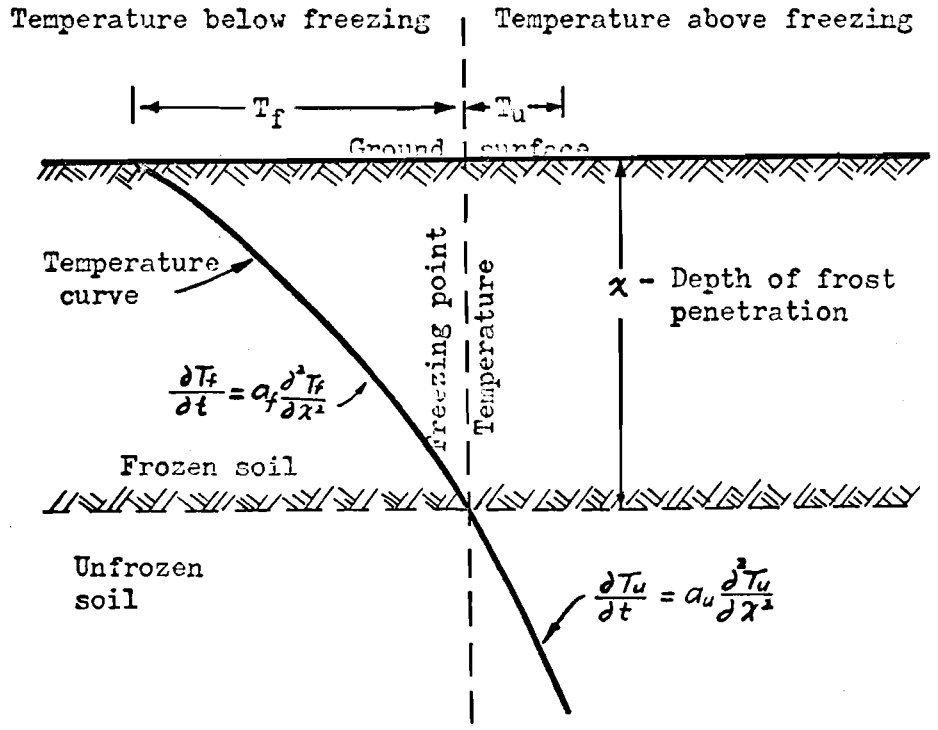

Fig. 12 - Ground temperature profile for modified Berggren Model.

Similarly, in the unfrozen soil layer,

$$\frac{\partial T_u}{\partial t} = a_u \frac{\partial^2 T_u}{\partial y^2} , \qquad (31)$$

where:

$a_f = K_f / C_f$ is diffusivity coefficient in frozen soil,

$a_u = K_u / C_u$ is diffusivity coefficient in unfrozen soil.

At point "A" on the frost front, the equation of continuity may be used. That is, the net rate of heat flow from the frost front must be equal to the latent heat supplied by the soil water as it freezes to a depth Δy in time Δt.

Hence,

$$L_h \frac{dy}{dt} = q_h , \qquad (32)$$

where:

q_h is the net rate of heat flow at the frost interface. So that,

$$K_f \frac{\partial T_f}{\partial y} - K_u \frac{\partial T_u}{\partial y} = L_h \frac{dy}{dt} . \qquad (33)$$

The solution of y has been given by Aldrich (1956) as:

$$y = \lambda \sqrt{\frac{48 K_h F_t}{L_h}} . \qquad (34)$$

The correction λ depends on the thermal properties of both the frozen and unfrozen soils.

FORMATION OF ICE IN SOIL

In general, when the temperature of the water at a point drops below the freezing point, ice crystals will begin to form. The type of ice formation depends on the rate of freezing and the chemical properties of the soil. There is considerable movement of water in vapor and liquid form towards the point of freezing due to vapor pressure gradients and other pressure gradients.

Hogentogler (1937) reported that the formation of ice layers in completely saturated permeable soils may be accounted for by the fluctuation in the depth of the frost line. This is due to the change in air temperature when the temperature remains below the freezing point.

As shown in Figure 13, "A" represents a column of unfrozen soil. With a drop in temperature the frost line penetrates as shown in "B", and the soil freezes, resulting in a heave equal to the moisture expansion of 9 percent. When temperature rises, the under portion of the frozen layer melts and returns to normal volume, thus leaving a crevice under the frozen layer equal in thickness to 9 percent of the original thickness of the water in the portion thawed. This crevice then fills with water as shown in "C", and on the next temperature drop becomes an ice layer as shown in "D". A repetition of this process produces a second crevice and ice layer as shown in "E" and "F".

Yong and Warkentin (1966) analyzed how ice layers form in coarse and fine-grained soils under freezing temperatures. In coarse-grained soils (granular) soils, because of the size of the particles, the gravity forces have an effect both on the mineral and liquid phases. The surface forces are, by comparison with the gravity forces, so small that their effect may be neglected. Thus, the bulk of the water in a saturated granular soil may be considered as free water. When such a soil-water system freezes, the ice can penetrate from one void into the next. That is, water in the soil voids freezes as individual ice crystals without movement of water to points of ice crystallization. Both experimental investigations and field studies indicate little or no heaving of soils as a result of freezing in a granular soil-water system.

The beginning of ice growth in a saturated soil-water system composed of coarse-grained particles may be thought of as ordinary freezing of water within the interspaces of the porous soil mass. Growth of the ice crystal will progress as long as the energy available due to heat transfer is greater than the ice-water interfacial pressure energy. The ice-water interfacial pressure P_{iw} depends on the curvature of the freezing plane and on a constant which is related to the interfacial energy between water and ice. The equation for P_{iw} is given as;

$$P_{iw} = C_{iw} \left(\frac{1}{r_1} + \frac{1}{r_2} \right) , \qquad (35)$$

where:

C_{iw} is a constant depending on interfacial energy between water and ice,

r_1, r_2, are principle radii of curvature of the curved interface.

The above equation is very similar to the interfacial pressure equation.

The energy available due to temperature depression or heat transfer may be examined in terms of thermodynamics. Assuming a closed univariant system, then the second law of thermodynamics can be expressed as:

$$F = Q_h \frac{T_1 - T_2}{T_2} , \tag{36}$$

where:

F is free energy or energy available,

T_2, T_1 are ice and water temperature respectively,

$Q_h \simeq L V_w$, since the heat transferred from T_2 to T_1 excluding L_h is small.

Equation (36) may be written in the form of pressure or suction if F is divided by the volume V. Thus

$$\frac{F}{V} = H_S = L_h \left(\frac{T_2 - T_1}{T_2}\right), \tag{37}$$

where:

H_S is soil suction.

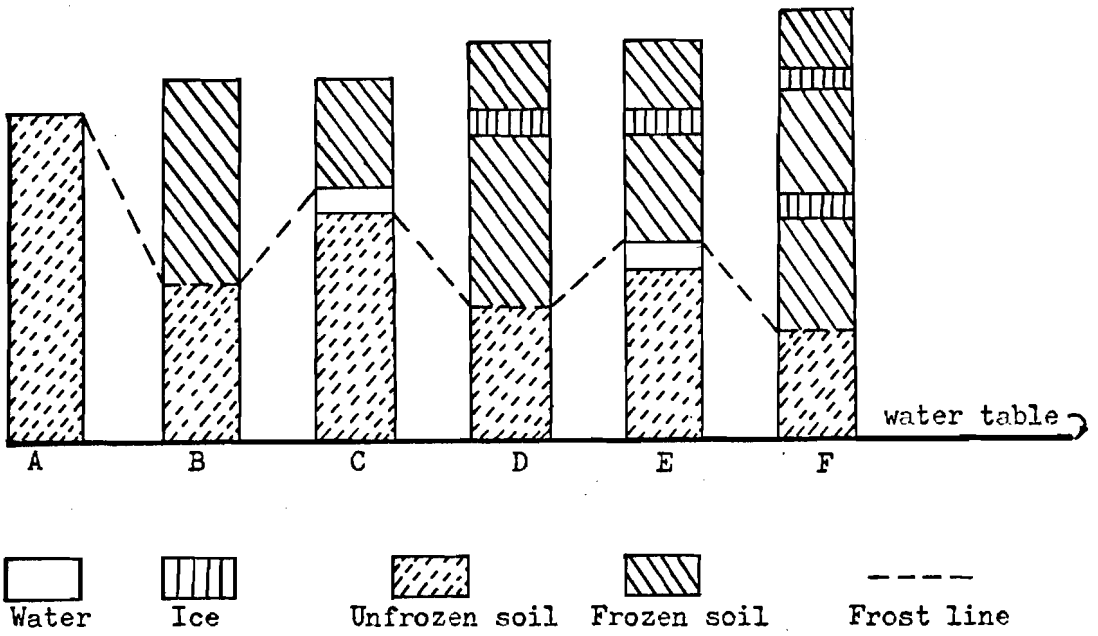

Fig. 13 - Ice layer formed by fluctuations in frost line.

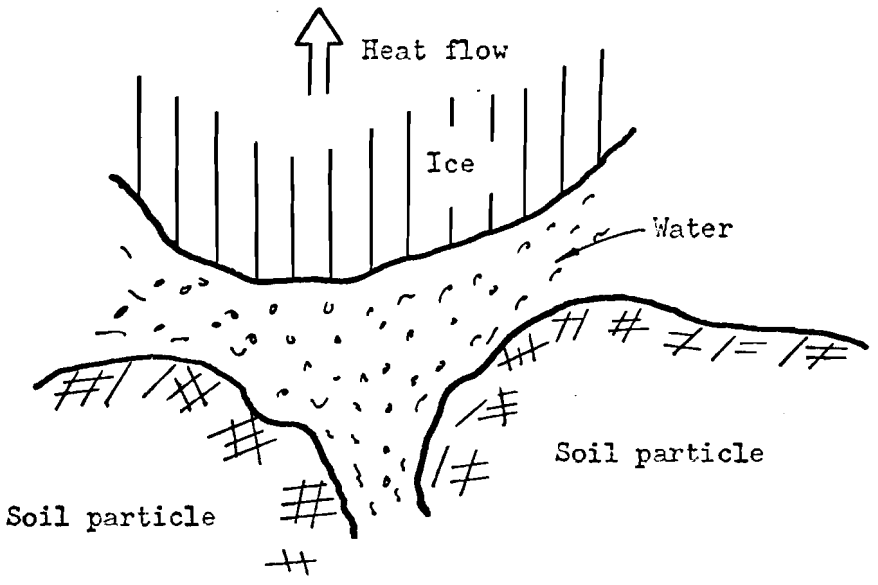

Fig. 14 - Schematic diagram of ice front and curvature of freezing plane.

As long as H_s is greater than P_{iw}, freezing of the pore water in a saturated granular soil mass will continue. H_s is a measure of the matric and osmotic potentials. For granular soil, the osmotic potential is insignificant. Hence H_s reflects the matric potential.

It is likely that each void space in the soil mass would contain one or more ice crystals. The formation of ice crystals may occur on the basis of both heterogeneous and homogeneous nucleation. Heterogeneous nucleation is initiation of growth or formation of an ice crystal by a foreign substance and homogeneous nucleation is initial growth on the basis of a bud of crystallization formed within the water phase.

If water within the soil mass is supercooled suddenly, spontaneous nucleation would likely occur. The soil-water system would freeze instantaneously, giving rise to multicrystal formation. If nonspontaneous nucleation were to occur, fewer crystals would be formed and the ice mass would be composed of large crystals. All of those will depend on factors such as temperature and duration of freezing.

Figure 15 shows a schematic view of soil freezing in a coarse-grained soil-water system. The system is assumed to be completely saturated and in this case the uniaxial direction of freezing is a valid assumption.

The frost line is not necessarily a straight horizontal line because several physical properties of the soil mass have to be

considered. The water in the soil pores immediately behind the frost line is supercooled and will nucleate when the frost line advances further.

When fine-grained soils expand due to freezing, the volume may increase 100 percent as a result of formation of lenses of ice in the subsoil.

In order to explain the phenomenon of ice lens growth, the water surrounding the soil particles may be classified into two types:

a. Water absorbed by the soil particle,

b. Free or bulk water.

The distinction between these two classes is shown in Figure 16 but the actual separation between the two classes of water is indistinct and cannot be readily measured.

Adsorbed water is always affected by the forces associated with soil particles so that nucleation is most likely to occur in the free water. When nucleation and subsequent crystallization occur in the free water portion, growth continues as long as heat loss exceeds heat gain. Unless heat loss from the buds is equal to or greater than the heat gain from water brought in to the bud to foster growth, subsequent melting would occur. If heat loss is equal to heat gain, equilibrium is maintained.

Yong and Warkentin also state when all the free water in the pore space is used up for crystal growth, either one or both of two things must happen if further growth is to occur.

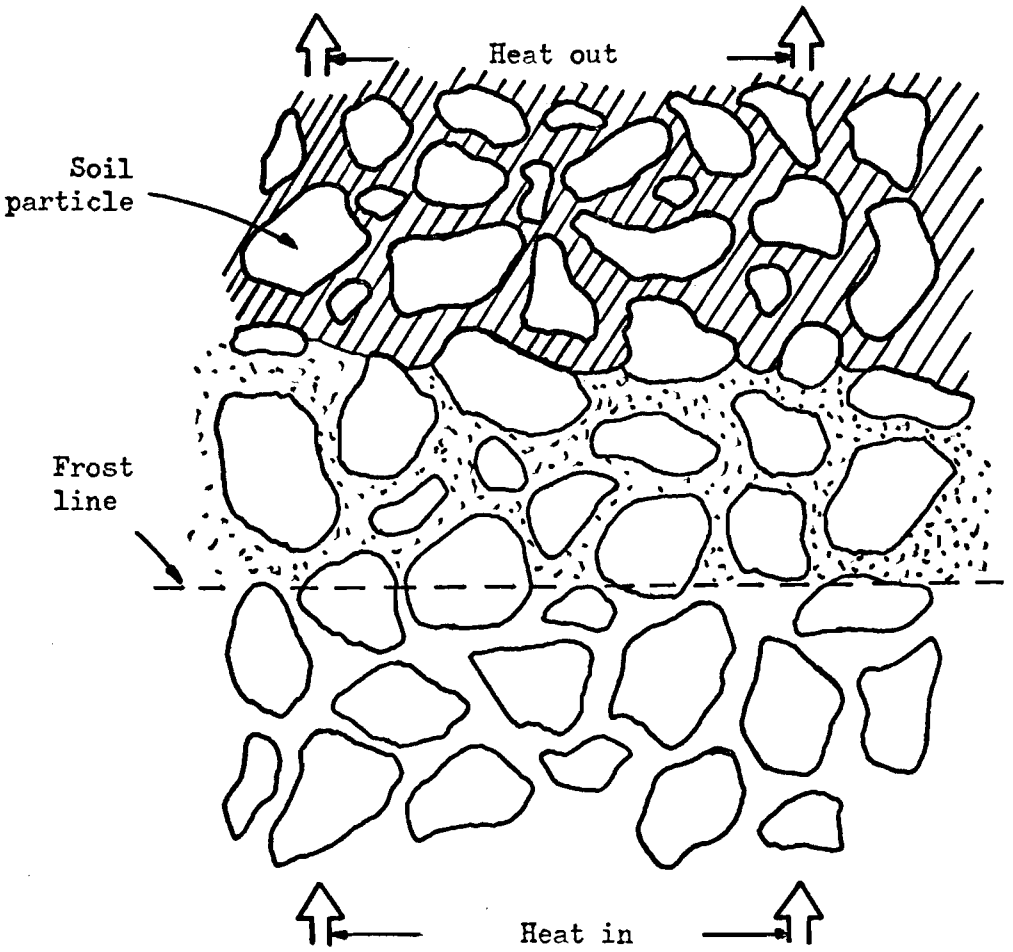

Fig. 15 - Schematic view of soil freezing in coarse-grained soils.

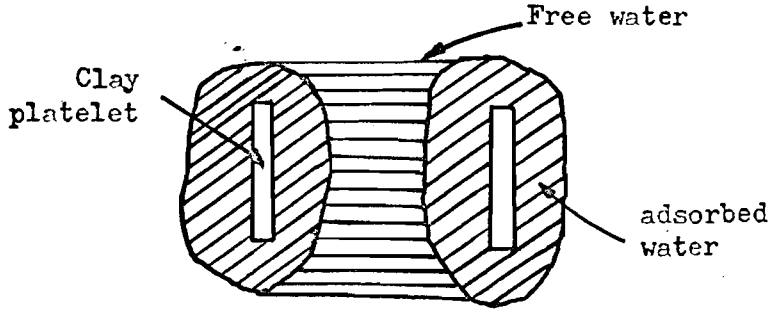

Fig. 16 - Schematic picture of the two classes of water in a saturated fine-grained soil.

a. The adsorbed water would be used for further growth.

b. More free water is drawn to the bud of crystallization from lower unfrozen layers of the soil.

Either of these processes will require greater energy; that is, the temperature must be further depressed. As the temperature is decreased, a pressure deficiency is induced at the ice front. Whether this deficiency in pressure is sufficient to move water to the growing bud or not will depend on the availability of the free water in adjacent pores and of the adsorbed water. Freezing continues until the energy required to bring in water to keep growing becomes too large and growth stops. Then another nucleus would be formed farther ahead of the ice front.

The pictorial sequence for growth of ice lenses is presented in Figure 17.

In stage 1, the bud of crystallization is formed in the free water. If the heat balance conditions are satisfied, the ice crystal will grow until all the free water within this pore space is added to the growing crystal. When all the free water in the pore has been used up, as shown in Stage 2, free water is drawn from the adjacent pore, and water under the influence of the particles is also used to add to ice growth. Particle displacement occurs as a result of both water loss and crystal growth.

With further temperature decreases, more particle displacement occurs as water is drawn from sources farther away from the bud of crystallization, and the ice crystal grows. This is shown in Stage 3.

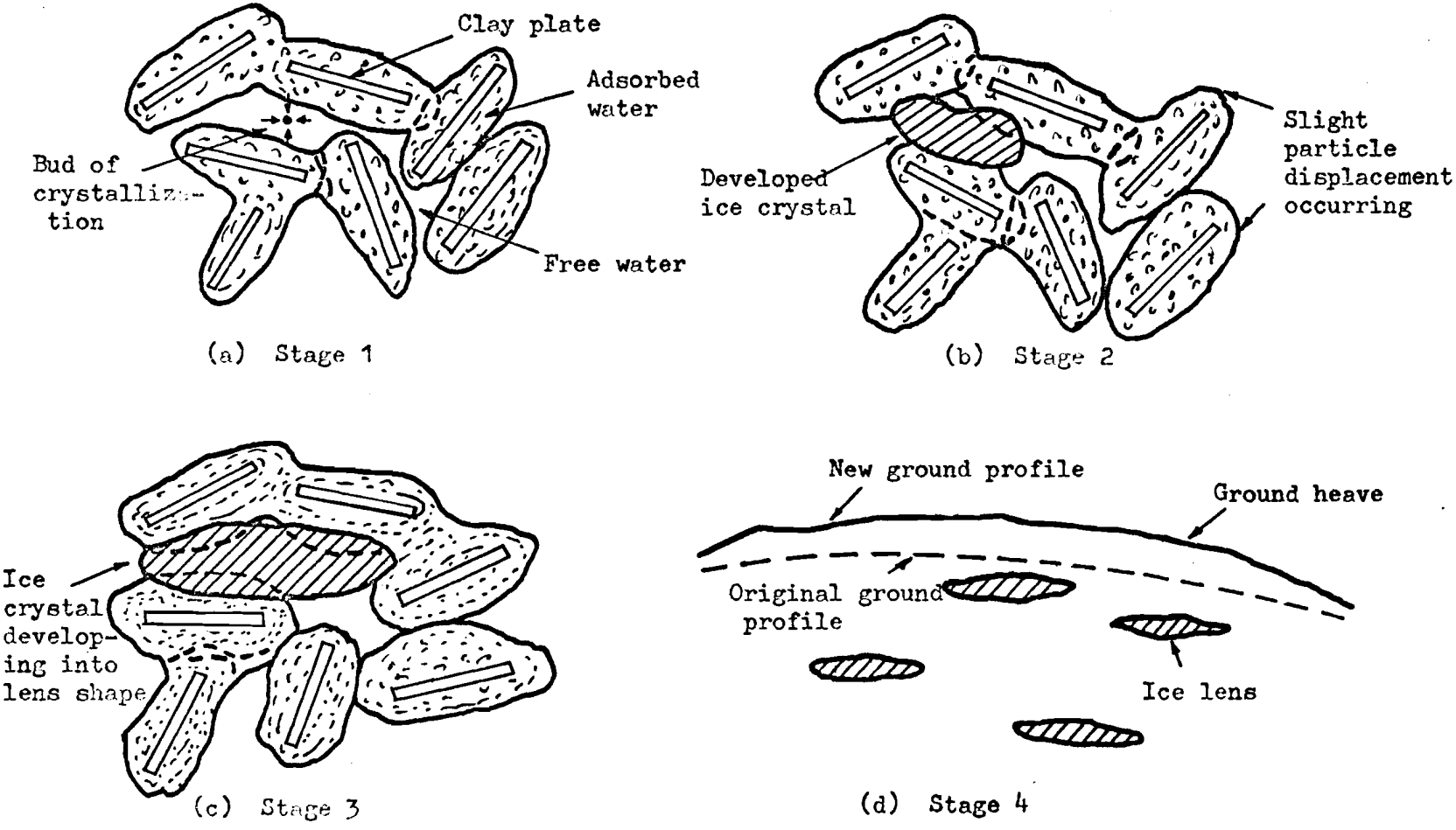

Fig. 17 - Stages in growth of ice lenses.

Since heat transfer is essentially upward, the crystal begins to develop such as to form a horizontal ice lens. If the growth of the ice lens is to continue, the temperature must be decreased further and the heat transfer must consequently be much greater. The more the water in the immediate pore space is held to the soil particles, the more free water from adjacent pores must be drawn up to the ice lens.

Stage 4 of the growth of an ice lens occurs when all the available water within the neighboring area has been used up and a further supply is not available because of the high energy requirements. When this happens, another lens will begin to grow lower down in the same way. The process will be repeated as long as the cold front moves downward and water is available.

PERMEABILITY

In order to determine the effect of moisture content and soil type on the permeability it is necessary to freeze soil samples at a particular moisture content and then measure the permeability. It is not possible to use water for these permeability measurements, since if the water is at a temperature above freezing the ice in the soil sample would melt and the permeability would not be constant.

It was therefore necessary to use a fluid which has a lower freezing temperature than water to measure the permeability. It was decided to use air for the measurement as the equipment could be placed in a cold room and isothermal conditions could be maintained.

A steady state measurement with air is not practical, since the measurement of the quantity of air is rather difficult. A non-steady state analysis is possible however, that is somewhat analogous to that used in the case of the falling head permeameter, used for laboratory measurements of permeability with water.

In the case of unsteady flow of air a closed tank is used for the supply. Knowing the pressure at the beginning and the end and the volume of the tank, it is possible to calculate the volume of air from Boyle's law.

The development of the expression for permeability by this method was originally done by Kirkham (1946).

According to Darcy's law,

$$q = - \frac{K_a}{\mu} \frac{P - P_a}{L}$$

where:

q is velocity of flow,

K_a is permeability coefficient for air,

μ is absolute viscosity of air,

P is pressure in the supply tank at any time,

P_a is atmospheric pressure,

L is the length of the sample.

The velocity, q, is the volume of flow in an increment of time, dt, divided by the cross-sectional area of flow, or,

$$\frac{V_{a1} - V_{a2}}{dt} = - \frac{A K_a}{\mu} \frac{P - P_a}{L} \qquad (38)$$

where V_{a1} is the volume of the air initially in the tank at atmospheric pressure,

V_{a2} is the volume that the air in the tank at time t_2 would have at atmospheric pressure.

By Boyle's Law

$$P_1 V = P_a V_{a1} \qquad (39)$$

and

$$P_2 V = P_a V_{a2} \qquad (40)$$

where V is the volume of the tank,

P_1 is the initial pressure in the tank,

P_2 is the pressure in the tank at time t_2.

Combining equations (39) and (40)

$$V_{a1} - V_{a2} = \frac{P_1 V}{P_a} - \frac{P_2 V}{P_a} \qquad (41)$$

$$= \frac{V}{P_a} dP$$

where dP is an increment of pressure.

Substitution into equation (38) and rearranging, we obtain

$$\int_{P_1}^{P_2} \frac{V\,dP}{P_a (P - P_a)} = - \frac{A K_a}{L \mu} \int_{t_1}^{t_2} dt$$

Integrating and solving for K_a ,

$$K_a = \frac{L V \mu}{A P_a} \left(\frac{\ln P_1/P_2}{t_2 - t_1} \right)$$

As shown in Figure 18 the pressure measurement is done with a mercury manometer so the pressure ratio is

$$\frac{P_1}{P_2} = \frac{y_1 (\gamma_{Hg})}{y_2 (\gamma_{Hg})}$$

$$= \frac{y_1}{y_2}$$

Changing to logarithms to the base 10 this can be written as

$$K_a = \frac{2.30 L V \mu}{A P_a} \left(\frac{\log_{10} y_1 - \log_{10} y_2}{t_2 - t_1} \right)$$

$$= \frac{2.30 L V \mu}{A P_a} S'$$

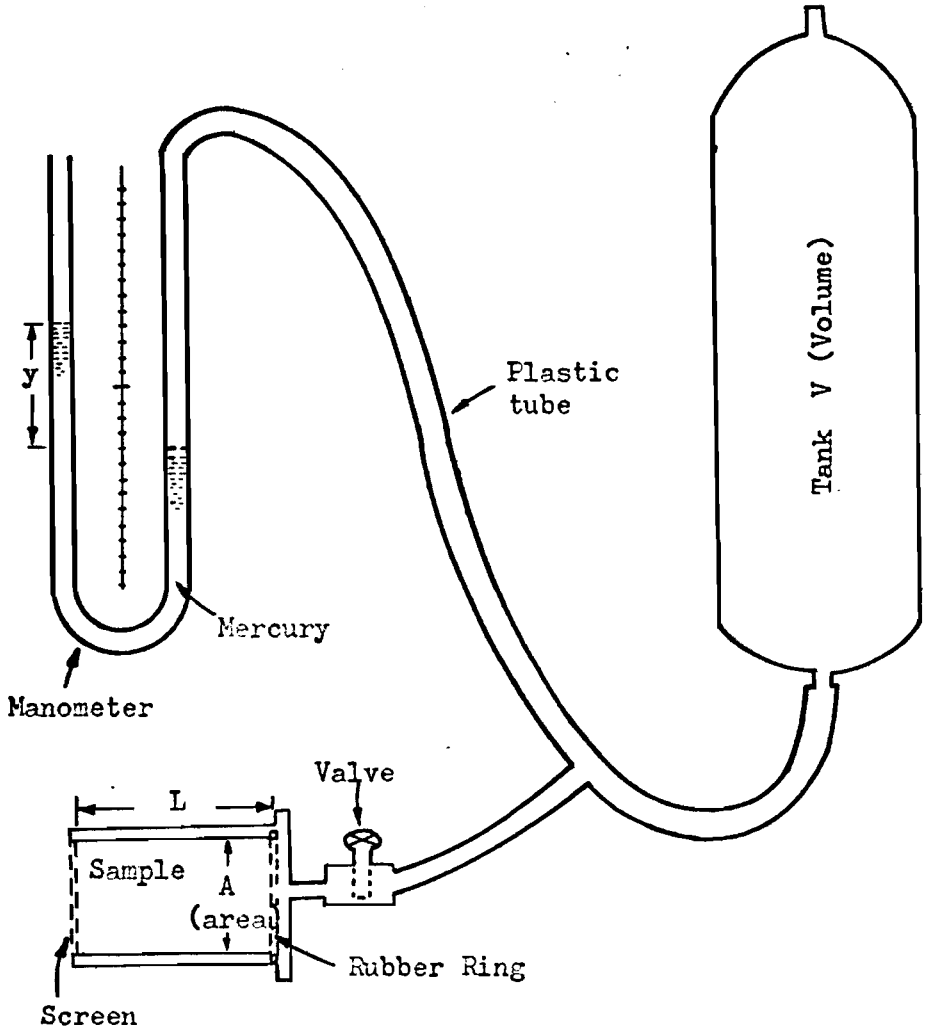

Fig. 18 - Schematic diagram of the equipment.

where S' is the slope of a $\log_{10}$ y versus time curve.

CHAPTER IV

EXPERIMENTAL PROCEDURE

In the laboratory, it would be very difficult to attempt to investigate all the soil moisture conditions and soil types that lead to the formation of ice lenses as considered in the literature review.

For this reason every effort was made to eliminate the formation of ice lenses in the soil columns. This was done by freezing the samples from all sides and as quickly as possible.

This was felt to be justified since the low infiltration rate which leads to floods is largely a surface phenomenon. Larin (1963) has reported that to a depth of 5 to 10 cm the infiltration rate does vary with variations in the air permeability of the layer.

Before testing the permeability of the frozen soil, it was necessary to determine some of the physical properties of the soil particles such as the particle size distribution and the specific gravity.

The particle size characteristics of the samples are shown in Table 1 and Figure 19. The standard sieves used included Nos. 100, 80, 48, 28, 14, and 8.

A Christian Becker specific gravity balance was used to determine the specific gravity of a hydrocarbon liquid which was then used to determine the specific gravity of the soil particles with standard procedures.

TABLE 1. PHYSICAL PROPERTIES OF SOILS

		Particle Size (% Smaller Than)					
Soil Type	Specific Gravity	0.0100"	0.0125"	0.0208"	0.0357"	0.0714"	0.1250"
Coarse Sand	2.616	4.86	7.03	15.40	38.89	73.65	95.48
Fine Sand	2.660	4.79	12.17	38.67	83.22	100.00	100.00
Silt	2.449	48.46	52.29	60.03	70.69	83.33	100.00

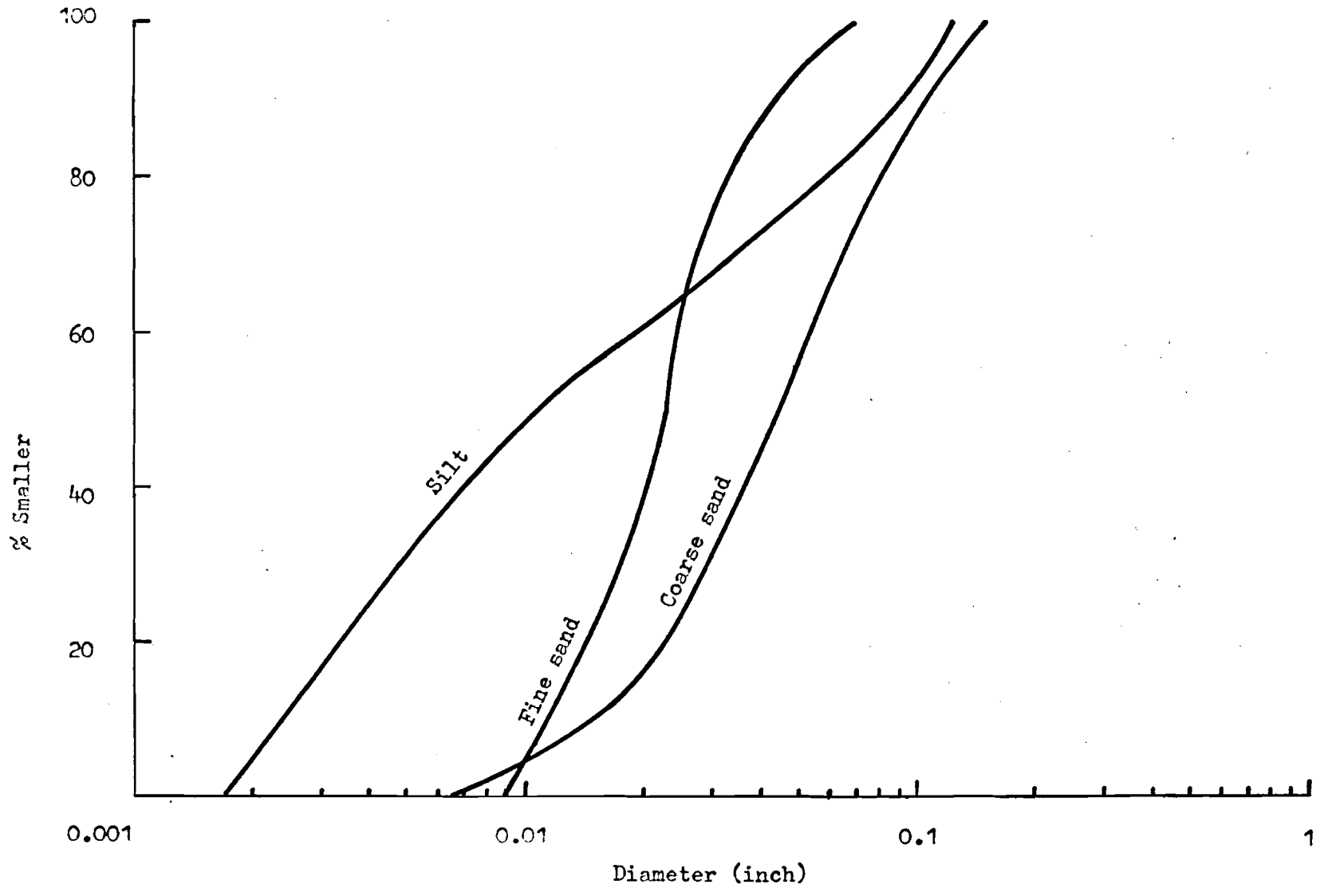

Fig. 19 - Particle-size-distribution curves

The equipment for testing the permeability of frozen soil is shown in Figure 20. A schematic diagram of the equipment showing the manometer, valves and air tank (1000 cu in.), is shown in Figure 18.

When preparing the soil for freezing, the soil sample was first mixed thoroughly with water in a Hobart A-200 mixer (as shown in Figure 21), and packed in plastic columns of about 5, 10, and 14.5 cm long and 6.4 cm in diameter. Grooves were machined around the inside of the plastic cylinders at 2 to 3 cm intervals to prevent air from flowing along the wall. After packing the columns were covered with plastic paper to eliminate evaporation and were put in a freezer for about 24 hours before the permeability tests were conducted.

Air was first pumped into the tank with the hand pump and the air pressure in the tank was noted. The valve was opened and the timer was turned on. After a period greater than several seconds, the valve was closed and the time and the air pressure in the tank were recorded.

When all nine columns of soil were tested, the soil and moisture were weighed by an electric balance. The soil was then placed in a vacuum drying oven for at least 20 hours, after which the weight of dry soil was obtained.

The moisture in the soil was changed and the procedure was repeated to obtain the permeability at different values of saturation.

Fig. 20 - The testing equipment.

Fig. 21 - Hobart A-200 mixer.

CHAPTER V

RESULTS AND DISCUSSION

The experimental data are given in Tables 2, 3, and 4, and the values of permeability are plotted versus the parameter $\phi(1-S)$ in Figures 22, 23, and 24. This parameter was used because it gives an indication of the pore space that is available for flow of a fluid after the soil is frozen. In the experimental work this fluid was air but in a field situation it would be unfrozen water. From a theoretical standpoint there would be zero permeability when the parameter is zero since there would be no empty pores. From a practical standpoint the permeability should become zero before the parameter does since it is likely that the empty pores would not be interconnected at low values of $\phi(1-S)$. Low values of $\phi(1-S)$ are obtained either by having a small porosity or high saturation.

In Figures 22 and 23, it appears that there is a linear relationship between permeability and $\phi(1-S)$ when plotted on semi-logarithmic paper. The plotted lines are the best fit straight lines as determined by a least squares analysis. The equations for these lines are:

$$k_a = \exp\left[14.6\ \phi(1-S) - 6.03\right]$$

and

$$k_a = \exp\left[11.34\ \phi(1-S) - 6.69\right]$$

for coarse and fine sand respectively. The simple correlation coefficients are 0.866 and 0.950 respectively.

TABLE 2. PERMEABILITY DATA

Sample; Coarse Sand Sp. Gr. = 2.616

No. of Column	Length of Column cm	Cross-Section of Column cm^2	Porosity ϕ	Saturation S	Permeability $10^{-6} cm^2$	$\phi (1-S)$
1	4.996	25.538	.364	.532	.067	.170
2	5.034	23.735	.3774	.505	.069	.187
3	5.004	24.406	.3801	.523	.052	.182
4	10.170	23.894	.393	.490	.071	.201
5	10.378	23.869	.388	.491	.075	.198
6	10.418	24.305	.390	.481	.089	.203
7	14.486	24.317	.388	.454	.115	.211
9	14.397	24.812	.366	.406	.059	.257
1	4.996	25.538	.468	.249	.078	.187
2	5.034	23.735	.412	.313	.136	.283
3	5.004	24.406	.418	.301	.091	.292
6	10.418	24.305	.438	.278	.156	.316
7	14.486	24.317	.449	.263	.288	.331
8	14.298	25.513	.447	.267	.204	.328
9	14.397	25.812	.434	.281	.148	.312
2	5.034	23.735	.359	.716	.026	.102
3	5.004	24.406	.340	.780	.004	.075
4	10.170	23.894	.419	.558	.052	.186
5	10.378	23.869	.343	.764	.000	.086
6	10.418	24.305	.380	.666	.006	.127
7	14.486	24.317	.364	.717	.004	.103
8	14.298	25.513	.353	.744	.003	.091
9	14.397	25.812	.324	.845	.000	.050

TABLE 3. PERMEABILITY DATA

Sample: Fine sand Sp. gr. = 2.660

No. of Column	Length of Column cm	Cross Section of Column cm^2	Porosity ϕ	Saturation S	Permeability $10^{-6} cm^2$	ϕ (1-S)
1	4.996	25.538	.475	.252	.054	.356
2	5.034	23.735	.488	.241	.066	.370
3	5.004	24.406	.439	.292	.070	.311
4	10.170	23.894	.499	.236	.147	.382
5	10.378	23.869	.509	.226	.125	.394
6	10.418	24.305	.489	.248	.132	.368
8	14.298	25.513	.473	.254	.166	.353
9	14.397	25.812	.515	.215	.276	.404
1	4.996	25.538	.475	.103	.075	.426
2	5.034	23.735	.478	.163	.093	.400
4	10.170	23.894	.492	.165	.203	.410
6	10.418	24.305	.514	.091	.281	.467
9	14.397	25.812	.470	.110	.245	.419
2	5.034	23.735	.495	.120	.098	.436
3	5.004	24.406	.451	.142	.098	.387
4	10.170	23.894	.517	.111	.168	.459
5	10.378	23.869	.485	.124	.146	.425
6	10.418	24.305	.496	.120	.120	.437
7	14.486	24.317	.493	.120	.157	.434
8	14.298	25.513	.479	.127	.127	.418
9	14.397	24.812	.491	.121	.125	.432
3	5.004	24.400	.404	.575	.009	.172
5	10.378	23.869	.427	.527	.004	.202
8	14.298	25.513	.440	.387	.025	.270
1	4.996	25.538	.397	.964	.002	.014
3	5.004	24.406	.420	.867	.000	.056

TABLE 3. (Continued)

No. of Column	Length of Column cm	Cross Section of Column cm^2	Porosity ϕ	Saturation S	Permeability $10^{-6} cm^2$	ϕ (1-S)
6	10.418	24.305	.427	.764	.001	.101
7	14.486	24.317	.436	.806	.004	.083
8	14.298	25.513	.418	.844	.005	.005
9	14.397	25.812	.414	.848	.000	.063

TABLE 4. PERMEABILITY DATA

Sample: Silt Sp. gr. = 2.449

No. of Column	Length of Column cm	Cross Section of Column cm^2	Porosity ϕ	Saturation S	Permeability $10^{-6} cm^2$	ϕ (1-S)
1	4.996	25.538	.607	.168	.016	.499
2	5.034	23.735	.598	.177	.019	.493
3	5.004	24.400	.682	.150	.038	.580
4	10.170	23.894	.639	.141	.019	.549
5	10.378	23.869	.667	.127	.038	.582
6	10.418	24.305	.648	.137	.024	.560
7	14.486	24.317	.666	.124	.041	.584
8	14.298	25.513	.655	.131	.135	.569
9	14.397	25.812	.670	.123	.052	.588
1	4.996	25.538	.668	.295	.096	.471
2	5.034	23.735	.649	.330	.074	.435
3	5.004	24.406	.675	.293	.051	.477
4	10.170	23.844	.680	.288	.228	.484
5	10.378	23.869	.676	.293	.168	.478
6	10.418	24.305	.673	.298	.200	.472
7	14.486	24.317	.659	.302	.276	.460
8	14.298	25.513	.660	.306	.228	.458
9	14.397	25.812	.663	.299	.234	.465
1	4.996	25.538	.585	.562	.101	.256
2	5.034	23.735	.579	.574	.088	.247
3	5.004	24.406	.603	.524	.112	.287
4	10.170	23.894	.635	.454	.171	.329
5	10.378	23.869	.599	.526	.186	.284
6	10.418	24.305	.587	.597	.062	.236
7	14.486	24.317	.608	.495	.296	.307
8	14.298	25.513	.568	.585	.179	.236

TABLE 4. (Continued)

No. of Column	Length of Column cm	Cross Section of Column cm^2	Porosity ϕ	Saturation S	Permeability $10^{-6} cm^2$	ϕ (1-S)
9	14.397	25.812	.565	.588	.137	.233
2	5.034	23.735	.499	.952	.011	.024
3	5.004	24.406	.532	.624	.024	.200
4	10.170	23.894	.538	.626	.016	.201
5	10.378	23.869	.535	.851	.004	.080
6	10.418	24.305	.542	.742	.010	.140
7	14.486	24.317	.516	.919	.000	.042
8	14.298	25.513	.529	.830	.008	.090
9	14.397	25.812	.521	.647	.008	.184
1	4.996	25.538	.611	.501	.151	.305
2	5.034	23.735	.652	.389	.096	.399
3	5.004	24.406	.514	.743	.000	.132
4	10.170	23.894	.611	.506	.248	.302
5	10.378	23.869	.655	.385	.289	.403
6	10.418	24.305	.623	.475	.206	.328
7	14.486	24.317	.627	.469	.275	.333
8	14.298	25.513	.649	.395	.367	.393
9	14.397	25.812	.595	.560	.199	.262

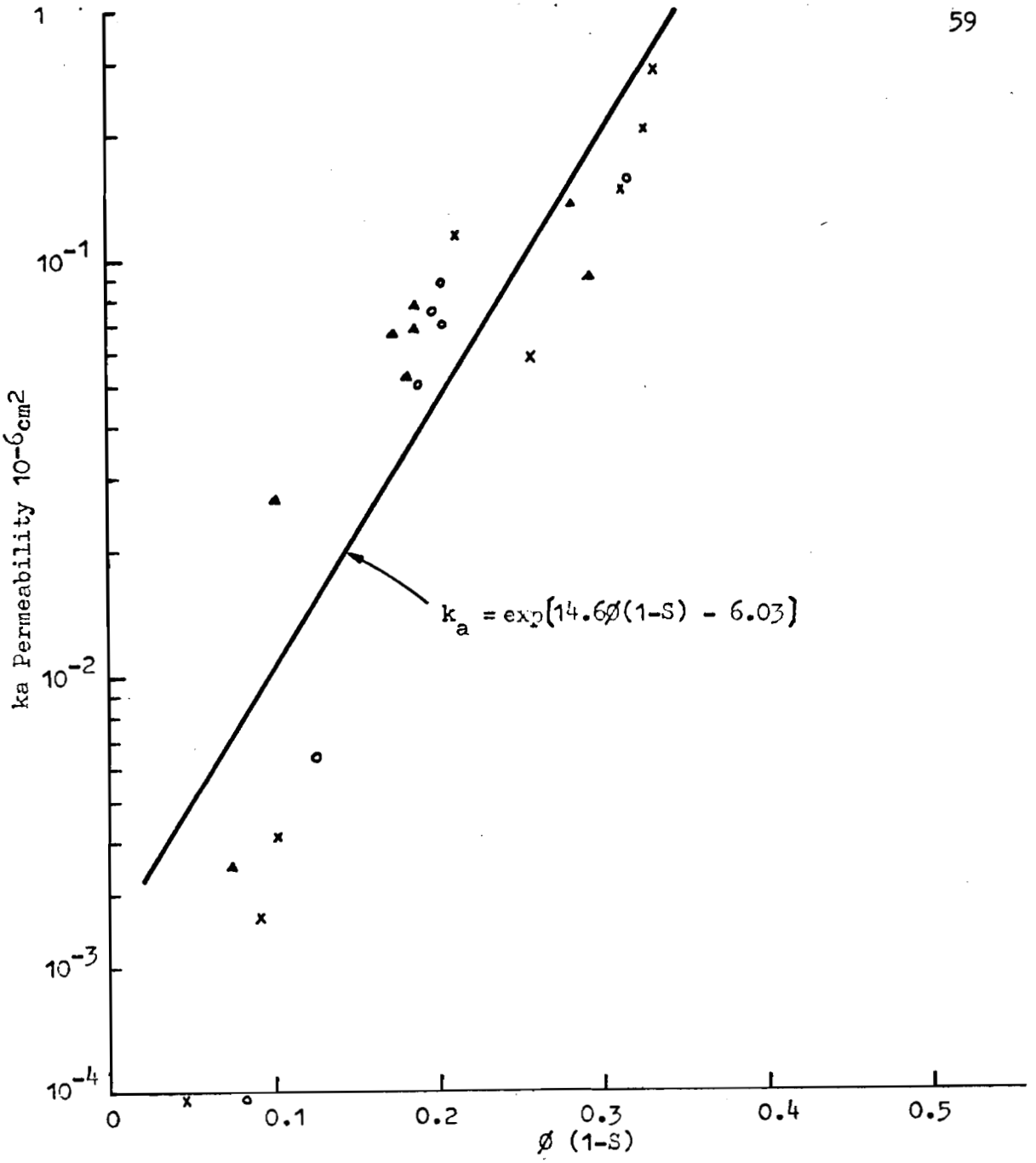

Fig. 22 - k_a vs $\phi(1-S)$ Relationship for coarse sand.

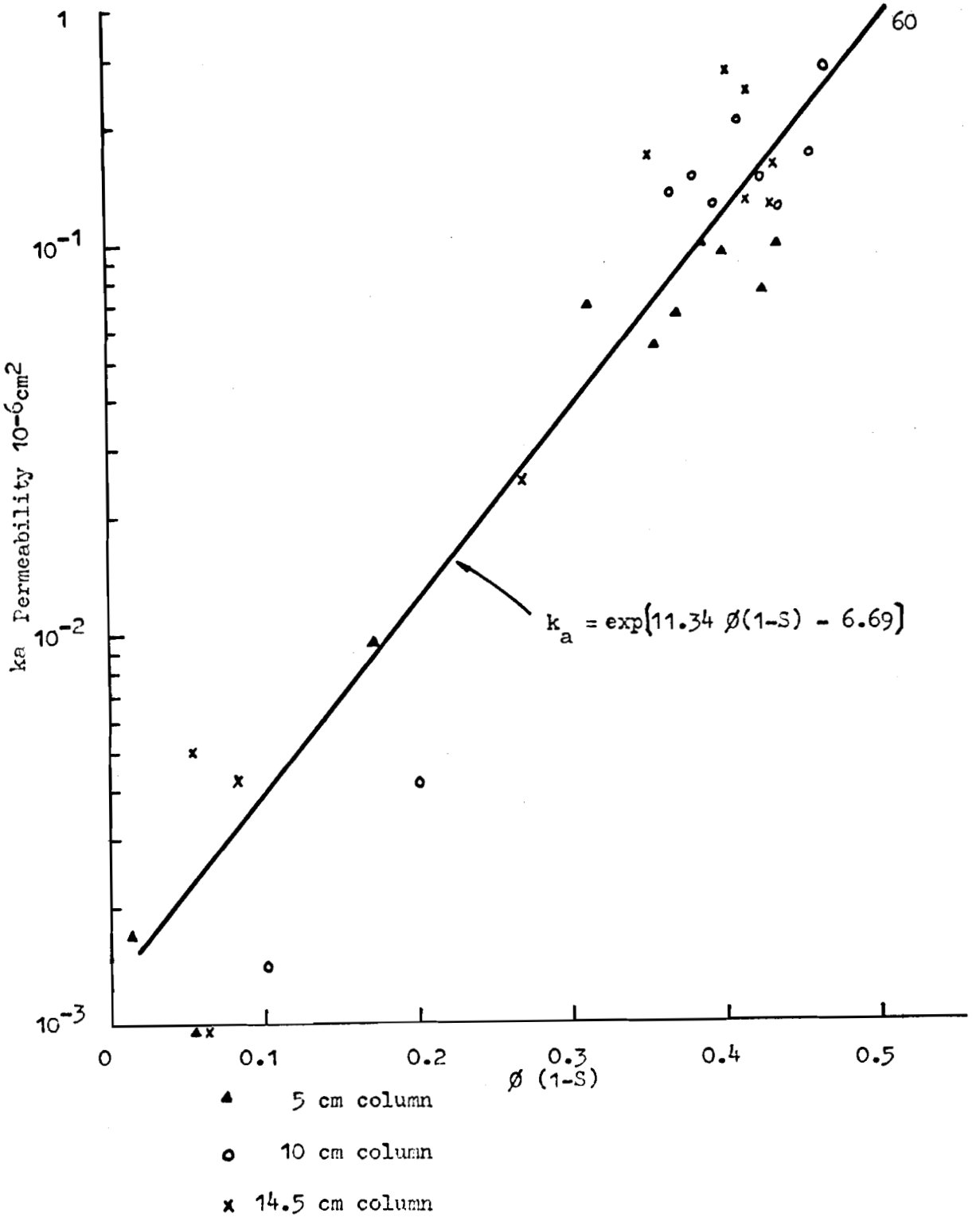

Fig. 23 - k_a vs $\phi(1-S)$ Relationship for fine sand.

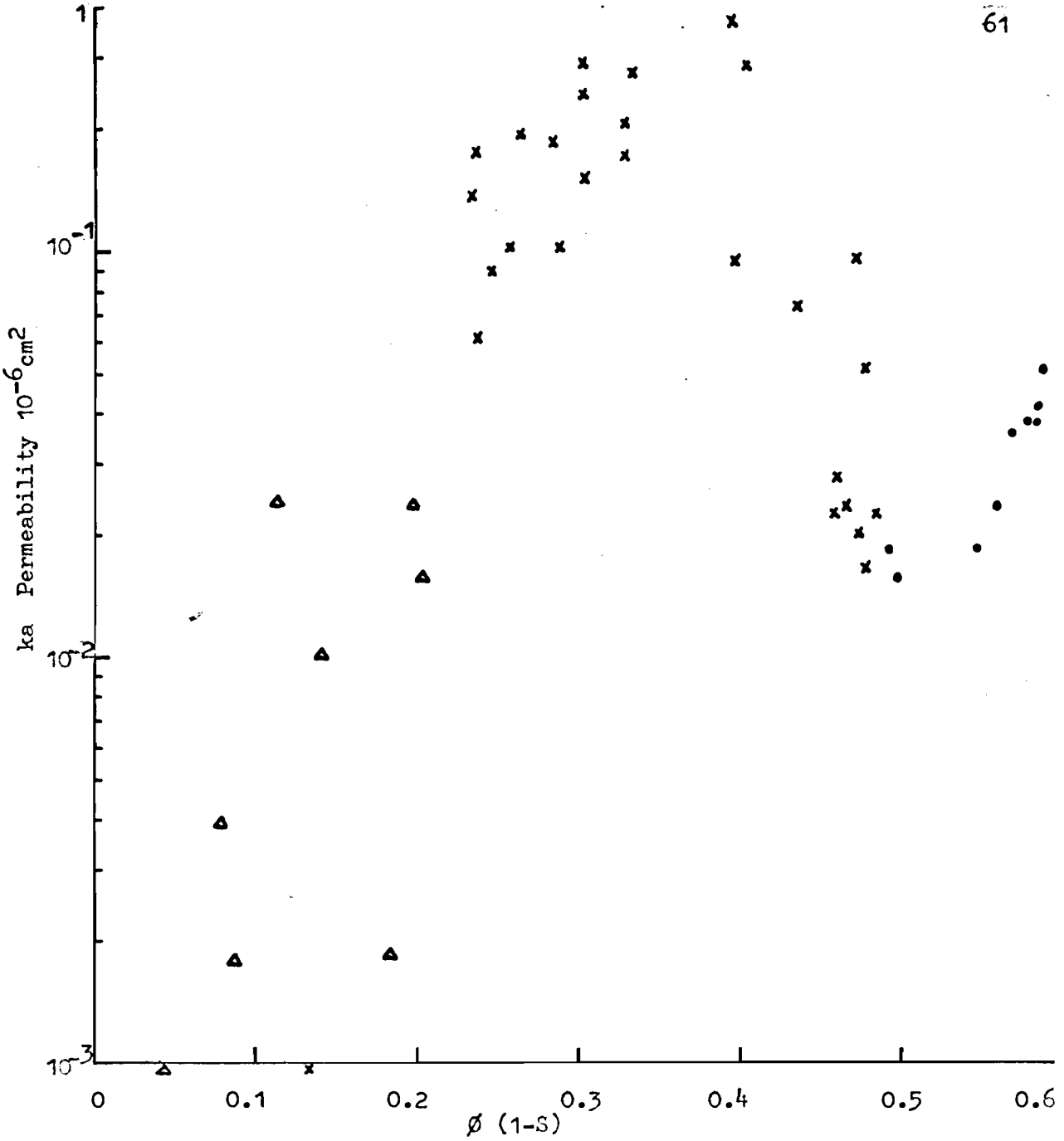

• Group 1 - undisturbed soil

× Group 2 - soil mixed with water

△ Group 3 - soil placed in column then wetted

Fig. 24 - k_a vs Ø(1-S) Relationship for silt.

For each of these curves there were several samples which had zero permeability and these points were not used in calculating the correlation coefficients. In all such cases the value of $\phi(1-S)$ was less than 0.13. Assuming that a reasonable value for the porosity of an undisturbed soil is 0.3, the saturation would have to be approximately 0.6 or greater for the soil to be impermeable when frozen. There are other samples which had significant permeability for values of the parameter less than 0.13.

For the silt (Figure 24) the data appear to be grouped in several areas. It is felt that this is due to the different procedures of wetting the soil and then placing it in the container. This procedure was very satisfactory for coarse grained material such as sand but was not satisfactory with silt due to forming aggregates which give non-uniform porosity. The data in group 1 were obtained when the silt was relatively undisturbed; after drying, rewetting and remixing, the other points were obtained. The larger than expected values of permeability are almost certainly due to large pores occurring between aggregates.

In general there is considerable scatter in all the experimental data; however, according to the correlation coefficients, 90 and 75 percent of the variation in fine and coarse sand respectively is accounted for by the one parameter which is felt to be good for the first attempt at this type of experiment.

Several limitations should be noted before attempting to apply any of these relationships to a field saturation:

1. The permeabilities measured here are air permeabilities which may not be the same as water permeabilities due to slip flow and the so-called Klinkenberg effect. This effect gives a permeability for gases which depends on the pressure of the gas.

2. There was no attempt made in the freezing of the columns to duplicate field conditions in which ice lenses form. In fact, every effort was made to eliminate the formation of ice lenses and have homogeneous conditions throughout the sample. This was evidently accomplished since there was no significant difference between various length columns.

3. A rather limited range of soil types were used in the experimental work. Finer textured soils are harder to wet uniformly and are much more liable to have ice lenses. Therefore, different experimental procedures would have to be used in finer grained soils.

CHAPTER VI

CONCLUSIONS AND RECOMMENDATIONS

Based on the results shown previously, the following conclusions may be made:

1. It is possible to measure the permeability of frozen soil under isothermal conditions by using a fluid with a lower freezing point than water while keeping the temperature below $32^{\circ}F$.

2. The parameter ϕ (1-S) is directly related to the permeability by an exponential relationship. The permeability decreases as ϕ (1-S) decreases.

3. The value of the parameter ϕ (1-S) must be less than about 0.13 in silts and sands for the permeability to be zero when the soil is frozen.

Some aspects of this work which should be worked on in the future are:

1. Isothermal experiments using a liquid should be run to get better data of permeability of the frozen soil. If a liquid is used it is much simpler to set up a steady state measurement of permeability besides avoiding the Klinkenberg effect.

2. Non-isothermal experiments using water as the liquid should be run to obtain some information on the mass transfer of water from the solid to liquid state under controlled conditions.

3. Air permeameter measurements should be conducted in the field under conditions below freezing when the ground is frozen in order to

see whether the relationships developed here are valid in the field.

REFERENCES

Aldrich, H. P. 1956. Frost penetration below highway and airfield pavement. Highway Research Board Bulletin 135: 124-144.

Andersen, D. M. 1967. Phase composition of frozen montmorillonite water mixtures from heat capacity measurements. U. S. Army Cold Region Research and Engineering Laboratory. Hanover, New Hampshire. Research Report 218.

Auguatine, M. T. 1941. Infiltration runs on frozen ground. Soil Science of America Proceedings 6:435

Bertle, F. A. 1966. Effect of snow compaction on runoff from rain on snow. Bureau of Reclamation, U. S. Department of the Interior. A Water Resources Technical Publication. Engineering Monograph No. 35.

Brooks, R. H., R. C. Reeve. 1959. Measurement of air and water permeability of soils. Transaction of the American Society of Agricultural Engineering. Vol. 2:125-128.

Cary, J. W. 1963. Onsager's relation and the non-isothermal diffusion of water vapor. Journal of Chemical Physics 67:126-130.

Dirksen, C. 1964. Water movement and frost heaving in unsaturated soil without an external source of water. Ph.D. Thesis, Cornell University.

Frederick, A. B. 1966. Effect of snow compaction on runoff from rain on snow. A Water Resources Technical Publication Engineering Monograph 35. Bureau of Reclamation, U. S. Department of the Interior.

Gardner, W. R. 1959. Solutions of the flow equation for the drying soils and other porous media. Soil Science Society of America Proceedings. Vol. 23:183-187.

Gerdel, R. W. 1954. The transmission of water through snow. Transaction, American Geophysical Union. Vol. 35:475-485.

Gold, L. W. 1963. Influence of the snow cover on the average annual ground temperature at Ottawa, Canada. I. U. G. G. Berkley Assembly. International Association Science Hydrological Publication No. 61:82-91.

Gold, L. W. 1967. Influence of surface conditions on ground temperature. Canadian Journal of Earth Science Vol. 4:199-208.

Gurr, C. G., T. J. Marshall, and J. T. Hutton. 1952. Water movement in soil due to a temperature gradient. Soil Science Vol. 24: 335-344.

Haupt, H. F. 1967. Infiltration, overland flow, and soil movement on frozen and snow-covered plots. Water Resources Research Vol. 3: 145-161.

Hoekstra, P. 1966. Movement in soils under temperature gradients with the cold side temperature below freezing. Water Resources Research Vol. 2:241-250.

Hoekstra, P. 1967. Moisture movement to a freezing front. Extract of Geochemistry, Precipitation, Evaporation, Soil Moisture, Hydrometry. General Assembly of Bern. by Cold Regions Research and Engineering Laboratory. U. S. Army Material Command. Hanover, New Hampshire.

Hogentogler, C. A. 1937. Engineering properties of soil. McGraw-Hill Book Company, Inc. New York.

Hole, C. E. 1950. Some observation on soil freezing in forest and range lands of the pacific northwest. Pacific Northwest Forest and Range Experiment Station Research Note 66.

Kirkham, D. 1946. Field method for determination of air permeability of soil in its undisturbed state. Soil Science Society of American Proceedings. Vol. 11:93-99.

Larin, P. A. 1963. Air permeability of frozen soils as a function of autumn plowing and moisture. Soviet Soil Science translation: 158-163.

Morozov, G. A. 1967. Computation of the change in the density of snow cover under the influence of water vapor diffusion, convection, sublimation and condensation in it. Translated from Russian, Meteorology and Hydrology No. 6:98-103.

Mosiyenko, N. A. 1958. Water permeability of frozen soil under condition of the Kulunda Steppe. Soviet Soil Science:1049-1053.

Schofield, R. K. 1935. The pF of the water in soil Transactions International Congress Soil Science, Vol. 2:37-48.

Slater, C. S. 1957. Cylinder infiltrometer for determining rates of irrigation. Soil Science Society of America Proceedings, Vol. 21:457-460.

Smith, W. O. 1943. Thermal transfer of moisture in soils. Transaction, American Geophysical Union. 24:511-523.

Stoeckeler, J. J., and S. Weitzman. 1960. Infiltration rates in frozen soils in Northern Minnesota. Soil Science Society of America Proceedings, Vol. 24:137-139.

Terzaghi, K. 1952. Permafrost. Journal of Boston Society of Civil Engineering. Vol. 39:1-50.

Trimble, G. R. Jr., R. S. Sartz, and B. S. Pierce. 1958. How types of soil frost affects infiltration. Journal of Soil and Water Conservation. 13:81-82.

U. S. Army Corps of Engineers, January 5, 1960. Runoff from snowmelt. Manual EM-110-2-1406, Washington, D. C. U. S. Government Printing Office, P. 10.

U. S. Army Corps of Engineers. 1963. February 1962. Floods in Southeastern Idaho. U. S. Army Engineering District, Walla Walla.

U. S. Army Corps of Engineers. 1966. Postflood Report. U. S. Army Engineering District, Walla Walla.

Woodside, W., and J. M. Kuzmak. 1958. Effect of temperature distribution on moisture flow in porous materials. Transaction, American Geophysical Union. 39:676-680.

Yong, R. N., and B. P. Warkentin. 1966. Introduction to soil behavior. The Macmillan Company, New York.